Science of the Total Environment 920 (2024) 170599

Contents lists available at ScienceDirect

Science of the Total Environment

journal homepage: www.elsevier.com/locate/scitotenv

Coarse-resolution burned area datasets severely underestimate fire-related forest loss

Amin Khairoun [a], Florent Mouillot [b], Wentao Chen [b], Philippe Ciais [c], Emilio Chuvieco [a,*]

[a] Universidad de Alcalá, Environmental Remote Sensing Research Group, Department of Geology, Geography and the Environment, Colegios 2, 28801 Alcalá de Henares, Spain
[b] Centre d'Ecologie Fonctionnelle et Evolutive CEFE, UMR 5175, CNRS, Université de Montpellier, Université Paul-Valéry Montpellier, EPHE, IRD, 1919 Route de Mende, 34293 Montpellier Cedex 5, France
[c] Laboratoire des Sciences du Climat et de l'Environnement, LSCE/IPSL, CEA-CNRS-UVSQ, Université Paris-Saclay, Gif-sur-Yvette, France

HIGHLIGHTS

- Sentinel-2 burned area detects higher fire-related loss than previous estimations.
- Fires contribute to 46 % of total forest losses in sub-Saharan Africa.
- Burned areas in Moist Tropical Forest are six times more likely to be deforested than unburned ones.

GRAPHICAL ABSTRACT

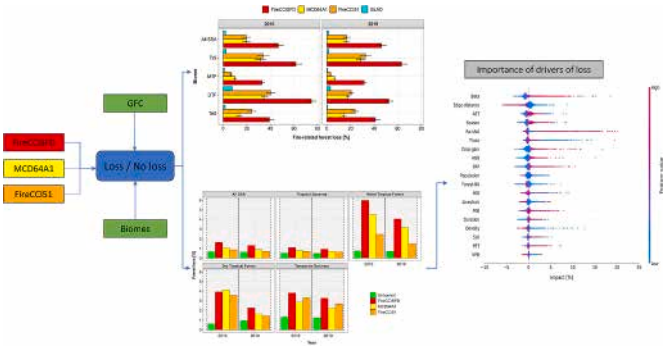

ARTICLE INFO

Editor: Manuel Esteban Lucas-Borja

Keywords:
Sentinel-2
Burned areas
Fires
Wildfires
Deforestation
Forest loss
Tropics
Africa
Satellite Earth Observation

ABSTRACT

Global coarse-resolution (≥250 m) burned area (BA) products have been used to estimate fire related forest loss, but we hypothesised that a significant part of fire impacts might be undetected because of the underestimation of small fires (<100 ha), especially in the tropics. In this paper, we analysed fire-related forest cover loss in sub-Saharan Africa (SSA) for 2016 and 2019 based on a BA product generated from Sentinel-2 data (20 m), which was observed to have significantly lower omission errors than the coarse-resolution BA products. Using these higher resolution BA datasets, we found that fires contribute to >46 % of total forest losses over SSA, more than twice the estimates from coarse-resolution BA products. In addition, burned forest areas showed more than twofold likelihood of subsequent loss compared to unburned ones. In moist tropical forests, the most fire-vulnerable biome, burning had even six times more chance to precede forest loss than unburned areas. We also found that fire-related characteristics, such as fire size and season, and forest fragmentation play a major role in the determination of tree cover fate. Our results reveal that medium-resolution BA detects more fires in late fire season, which tend to have higher impact on forests than early season ones. On the other hand, small fires represented the major driver of forest loss after fires and the vast majority of these losses occur in

* Corresponding author.
E-mail address: emilio.chuvieco@uah.es (E. Chuvieco).

https://doi.org/10.1016/j.scitotenv.2024.170599
Received 13 November 2023; Received in revised form 28 January 2024; Accepted 29 January 2024
Available online 2 February 2024

fragmented landscapes near forest edge (<260 m). Therefore medium-resolution BA products are required to obtain a more accurate evaluation of fire impacts in tropical ecosystems.

1. Introduction

Forests cover almost 30 % of the land surface and play a central role in the climate system through their association with core physical and biochemical processes, the hydrologic cycle, and atmospheric composition (Bonan, 2008). Forests are prone to several sources of disturbance and degradation leading to deforestation. Global gross forest losses are estimated at approximately 5 Mha yr^{-1} (Curtis et al., 2018). Fires have been identified as a critical driver of forest area loss (Curtis et al., 2018; Liu et al., 2019; van Wees et al., 2021), especially in the sub-Saharan African (SSA) continent, the most affected by fires. This region is responsible for over two-thirds of the global area burned (Lizundia-Loiola et al., 2020) and for more than half of the global pyrogenic greenhouse gas emissions (van der Werf et al., 2017). For these reasons, it was chosen as a priority to derive a continental burned area (BA) product at 20 m resolution based on the Multi-Spectral Instrument (MSI) onboard the European Space Agency's Sentinel-2 (S-2) satellite. A first version of this dataset was produced for 2016 using a single S-2 satellite (Roteta et al., 2019) and a more recent one for 2019 included the two S-2 satellites currently in operation (Chuvieco et al., 2022). The resulting product, named FireCCISFD20, was validated using a dedicated spatial sampling, obtaining significantly lower omission errors than for products based on coarse-resolution BA sensors (Chuvieco et al., 2022; Stroppiana et al., 2022).

Among fire impact assessments, large-scale estimations of fire-induced forest loss are very limited and associated with several sources of inconsistency. Some authors have linked the 30-m Global Forest Change (GFC) dataset with associated drivers based on reference samples (Curtis et al., 2018). These authors estimated that only 22 to 29 % of forest loss globally was related to fires, and much less in Africa (< 2 %). Crop cultivation was considered the main driver of deforestation in this continent, resulting from the increasing demand for agricultural products associated with the high rate of population growth (Rudel, 2013). However, these estimations generally ignore fire practices such as slash burning, which are commonly involved during conversion to agriculture (Doggart et al., 2020; van Wees et al., 2021). Due to the considerable challenge of accurately identifying slash-and-burn fires, the mentioned approach focused exclusively on large burn patches that were not followed by any subsequent conversion to cropland (Curtis et al., 2018). Consequently, the classification model's capacity to account for the contribution of smaller fires was constrained, acknowledging a substantial uncertainty. Additionally, the use of fire as a practice of conversion whether solely or jointly with other practices (e.g. mechanical cutting) is always leading to similar consequences in terms of Greenhouse Gas emissions, aerosol plumes, soil degradation (Davidson et al., 2008; Pellegrini et al., 2018) and biodiversity loss (Styger et al., 2007). These fire-enabled practices are significantly more damaging in comparison with fire-free conversion methods such as slash-and-mulch (Davidson et al., 2008) or agroforestry systems (Clark et al., 2016).

To account for all kinds of forest fire events, other authors aggregated the GFC data to the native resolution of global fire products (500 m) concluding with an overall estimation of fire-related forest loss of 20 % over SSA (Liu et al., 2019; van Wees et al., 2021). This estimation is deemed conservative since small fires are mostly undetected in coarse-resolution global BA products (Ramo et al., 2021). In fact, a significant increase of fire-related forest loss was reported, especially in the tropics, when active fire observations were used for BA estimations through a statistical model (van Wees et al., 2021). This approach provided a first estimation of 31 % of fire-related forest losses, yet omitting a large proportion of small, fast-spreading or low-intensity fires that the active fire sensor missed during the actual burning process.

In this study, we used more accurate BA information derived from a higher-resolution sensor to obtain improved estimations of fire-related forest loss, particularly in regions with frequent and fragmented fires such as SSA. We cross-analysed high-resolution (≤30 m) BA and forest cover loss datasets generated from satellite sensors for the SSA, and compared the results with previous estimations based on coarse-resolution (≥250 m) satellite data. We defined fire-related forest loss as any causal relationship where fire is associated with forest loss. This includes situations where fire and forest loss occur simultaneously (e.g. wildfires), cases where forest loss follows a fire event (e.g. tree mortality subsequent to fire damage), and instances where forest loss precedes fire but both occur in the same year and typically within a couple of weeks (e.g. slash-and-burn).

We examined, across different biomes (Dinerstein et al., 2017) of the whole SSA region, fire impacts on forest cover change, as estimated from two datasets: the Global Forest Change (GFC) v.1.8 (Hansen et al., 2013) and two years of the FireCCISFD BA products generated from S-2 MSI images at 20 m resolution. Fire impacts on forest loss were estimated from these BA datasets and compared, for the same years and area, with two global BA products based on MODIS data, namely MCD64A1 Collection 6 (at 500 m), the standard BA product of NASA (Giglio et al., 2018), and FireCCI51 (at 250 m), created within the European Space Agency's Climate Change Initiative (CCI) Programme (Lizundia-Loiola et al., 2020), the same as the FireCCISFD's, but with a different algorithm and sensor. A similar comparison was performed with the GLAD fire-related forest loss dataset developed by the Global Forest Watch, using a sample-based unbiased estimator of forest loss drivers (Tyukavina et al., 2022). Fire-related forest loss was analysed by biome and country, while the assessment of the relationship between fire occurrence and tree cover loss included three different factors influencing deforestation: seasonal patterns, fire energy released and distance to forest edges. We hypothesised that: 1) fires with higher released energy (Fire Radiative Power, FRP) would imply a higher chance of forest loss; 2) late-season fires would be more severe, as vegetation would be drier, and therefore more prone to deforestation or forest dieback, and 3) burning in fragmented landscapes located at forest edges is more likely to trigger forest loss due to light penetration and drier microclimate.

2. Materials and methods

2.1. Main input datasets

FireCCISFD products include two years of BA at 20 m resolution detected over SSA based on reflectance images acquired by the Multi-Spectral Instrument (MSI), onboard the S-2 satellite, complemented with active fire observations. The 2016 version, called FireCCISFD11, was generated from S-2A data in combination with the MODIS active fires (MCD14ML), whereas, the second version (2019), called FireCCISFD20, included images acquired by both S-2A and S-2B satellites in order to improve the revisit time from 10 to 5 days, while MODIS active fires were replaced with an active fire product derived from the Visible Infrared Imaging Radiometer Suite (VIIRS) sensor onboard the Suomi-NPP satellite (Schroeder et al., 2014) and NOAA-20. VIIRS offers higher spatial resolution for active fires (375 m) than MODIS (1 km). Although we performed the analysis with the two years of S-2 data, we mostly focused on 2019, since in this year the two S-2 satellites were in orbit (S-2B was launched in 2017), and therefore the product had lower omission and commission errors (8.5 and 15 %), than the 2016 product (26.5 and 19.3 %, respectively), which was based on a single S-2 satellite (Roteta et al., 2019; Stroppiana et al., 2022).

The BA algorithm for the two years have a similar structure, based on

multitemporal change detection over all cloud-free scenes and backs up to 4 previous images in the case where clouds are contaminating the observations. The NIR spectral band (8A) of S-2 MSI, and two spectral indices were used as input for the BA algorithm, the Mid-Infrared Burned Index (MIRBI) and the Normalized Burned Ratio 2 (NBR2). The BA detection process included four major steps. First, an unburnable mask was created based on the scene classification map, then, the three abovementioned variables in addition to their multitemporal difference were used to generate an initial burn classification by applying fixed thresholds. The outputs of this classification were later overlaid with the VIIRS Active Fire hotspots in order to obtain the confirmed burned pixels, which were used to compute regional thresholds. These thresholds were applied for producing the final BA classification using a two-stage procedure, high-probability seeds were first detected and then neighbouring burned areas with lower probabilities were mapped. Intercomparisons were performed against two common global BA products (Chuvieco et al., 2022; Roteta et al., 2019).

The coarse-resolution BA products were designed to provide global information on fire occurrence. They were generated by applying a hybrid approach combining MODIS active fire observations with a multitemporal change detection process. This process was carried out using a vegetation index based on MODIS SWIR bands at 500 m for MCD64A1 Collection 6 (Giglio et al., 2018), while MODIS 250 m NIR band was used in the case of FireCCI51 (Lizundia-Loiola et al., 2020).

As for the analysis of forest cover loss, tree cover layers were obtained from the Global Forest Change (GFC) v.1.8 dataset (Hansen et al., 2013). The GFC provides the fraction of forest tree cover of the year 2000 along with the annual changes (loss/gain) at a medium spatial resolution (30 m). This dataset was derived from Landsat 7 Enhanced Thematic Mapper Plus (ETM+) and Landsat 8 Operational Land Imager (OLI). Forest cover map was obtained by applying a 30 % threshold to convert the fraction of tree cover to a forest/non-forest binary layer similarly to previous studies (Hansen et al., 2020; Taubert et al., 2018). This binary layer was used as the baseline of forest extent in 2000, then the annual binary layers of forest loss/gain were used to update yearly tree cover extent and get the most recent one prior to the year of processing.

The spatial analysis was performed based on terrestrial biomes obtained from the Ecoregions2017 dataset (Dinerstein et al., 2017), which provides a map of Earth's 846 terrestrial ecoregions and 14 biomes. The SSA comprises 8 terrestrial biomes, however, due to the insignificant size of some of them, a reclassification to major biomes was performed. This reclassification was similar to the approach adopted by other authors (Boschetti et al., 2016; Franquesa et al., 2022; Padilla et al., 2014), except for tropical forests where the merging between dry and moist tropical forests obscured their significant differences in terms of fire activity and impacts caused by fuel moisture content and therefore they were kept discriminated (Table A.1).

2.2. Estimation of fire-related forest loss

Fire-related forest loss refers to the different situations where fire is directly linked with the process of tree cover loss. These losses include irreversible forest cover conversion as well as disturbances followed by regrowth. In addition to forest loss observed during the year of fire detection, several authors found a significant tree stand-replacement during the succeeding years (Liu et al., 2019; van Wees et al., 2021). To balance the trade-off between delayed fire-induced tree mortality and commission errors related to tree mortality caused by factors other than fire, one lag year of losses was taken into account, following the proposal of van Wees et al. (2021). For instance, to assess fire-related losses of 2019, forest losses of 2019 and 2020 were aggregated. The GFC dataset was resampled to the 20 m resolution using the nearest neighbour method in the case of FireCCISFD, while in the case of coarse-resolution BA products, it was aggregated to the native resolution of each product (500 for MCD64A1 and 250 m for FireCCI51). The three layers of fire-related loss were then aggregated to a 0.05° resolution grid. Finally, the average value was estimated using proportional weights corresponding to the gross forest loss within each grid cell. This procedure was implemented in order to minimize the dominance of cells with very low forest losses (i.e. up to 90 % experienced <0.05 % of losses).

Two calibration parameters served to compute uncertainty. The first concerns threshold values of tree cover fraction of GFC, in which 6 different values were assessed (1, 10, 20, 30, 40 and 50 %). The inclusion or exclusion of the lag year was the second parameter. Similar adjustments were also considered by Liu et al. (2019) and van Wees et al. (2021). The 95 % confidence interval was used in our study rather than the range between the minimum and maximum estimates.

The other parameter analysed at this stage was the fraction of loss in burned forest, which refers to the proportion of the total forest burned area that experienced a forest loss. Once again, the losses of the following year to fire event were considered as fire is assumed to be the main driver of loss in such case.

Due to the limited temporal resolution of medium-resolution satellite missions (~5 days for the two Sentinel-2 satellites and ~8 days in the case of using two Landsats), the comparison between fire and forest loss dates entails substantial uncertainties. Therefore, we consider forest loss as fire-related as long as they both occur in the same year or when fire precedes tree cover loss by one year (delayed mortality).

2.3. Modelling of fire-related forest loss drivers

In order to assess the factors driving fire-related forest loss, an Extreme Gradient Boosting model (XGBoost) (Chen and Guestrin, 2016) was implemented. The model linked four categories of variables to the fraction of forest loss at 0.25° grid cells, including fire traits, forest structure characteristics climatic variables and human factors. The model parameters were optimised using a 10-fold cross-validation approach and we used 80/20 train-test splits. To mitigate overfitting issues the "early_stopping_rounds" functionality was applied, which ceases the growth of trees once the log-loss stops decreasing.

Concerning fire traits, the total forest BA was aggregated and grid cells with <5 ha of total BA (i.e. <0.007 % of the cell is burned) were ignored as they represented insignificant statistics about fire regimes. Areas with frequent fires such as Tropical Savanna were expected to exhibit higher resistance to fires and lower proportions of losses (Hoffmann et al., 2003). The difference between burn day (BD) and the mid-fire season was calculated for each native pixel and then the aggregation to grid cells was performed using the 75th percentile. The rationale behind this aggregation was to assess the symmetry of BD distribution, and in particular, the prevalence of late-season fires, presumably leading to more severe impacts (Govender et al., 2006). Depending on the hemisphere, fire season considerably diverges. In general terms, the regular fire season extends from November to February in the Northern Hemisphere of SSA, while most fires in the Southern Hemisphere occur from June to September (Ramo et al., 2021). The remaining fire-related variables were derived after delineating fire patches (FPs). The main aggregation parameter to build these FPs is the maximum burn date time-gap between two neighbouring pixels that has been fixed at 6 days. As a first step, pixels sharing the same BD are grouped into clusters under an eight-neighbour queens adjacency scheme. Then clusters are aggregated into FPs to generate unique-ignition point FP as described in Oom et al. (2016).

Self-organized criticality (SOC) (Bak et al., 1988) has been widely used to explain the distribution function of fire sizes (Laurent et al., 2018; Malamud et al., 1998) following a power law:

$$N_{FP} = \alpha . {A_{FP}}^{-\beta} \quad (1)$$

where A_{FP} refers to the area of the fire patch, N_{FP} is the number of fire patches of a given size A_{FP}, α is a normalization constant and β (Beta

elsewhere in the paper) is the exponent of the power law or the slope of fire distribution function. A value of zero for Beta indicates constant fire size density, while a high value translates a high frequency of small fires with respect to large ones. This parameter was fitted at grid cells of 0.25° for fires larger than 1 ha. Fire density (Density) was calculated based on the number of FPs within each cell. Since small fires were predominant, a strong skewness of the mean fire duration was observed, and therefore, this variable was reformulated as:

$$Duration = \frac{Duration_{all} + Duration_{large}}{2} \quad (2)$$

where: $Duration_{all}$ is the mean duration in grid cell and $Duration_{large}$ is the mean duration of fires exceeding 100 ha.

The fire radiative power (FRP) was used as a proxy for fire intensity. FRP estimates the radiant heat power released by fires during the combustion process (Wooster et al., 2005). It was derived from VIIRS active fires, and aggregated to the modelling grid cell by using the median following Laurent et al. (2019). On the other hand, a detailed analysis of FRP distribution by BA product was performed. The corresponding value of FRP was attributed to burned pixels falling within 375-m buffer from each active fire, and in the case a pixel overlaps with several active fires (i.e. from different time observations), the maximum value of FRP was retained.

The impact of forest structure on forest loss was taken into account in the predictive model using two variables: the distance to forest edge (Edge-distance) and the Above-Ground Biomass (AGB). The former was generated by computing the proximity of fire events to the first non-forest pixel. The overall distribution of this feature was evaluated, and then aggregated by averaging. The AGB was derived from the ESA-CCI Biomass product (100-m) for the year 2018 (Santoro and Cartus, 2021) and was aggregated by averaging as well.

Climate-related explanatory variables were retrieved from the TerraClimate dataset (Abatzoglou et al., 2018), from which, six variables were included in the model, namely the annual rainfall (Rainfall, $mm{\cdot}yr^{-1}$), the annual mean maximum temperature (Tmax, °C), the annual actual and potential evapotranspiration (AET and PET, respectively in $mm{\cdot}yr^{-1}$), the annual soil moisture (Soil, $mm{\cdot}yr^{-1}$) and the annual mean vapour pressure deficit (VPD, $kPa{\cdot}yr^{-1}$). The Markham Seasonality Index (MSI) (Markham, 1970) was calculated based on the monthly precipitation. It describes the rainfall distribution over the year. A value of 0 % implies an equivalent distribution over the months, while 100 % indicates that all rainfall occurs in a single month. Monthly values are considered as vectors, where the magnitude is defined by the corresponding rainfall (Pm) and the direction, is defined by an angle θ_m. The 365 days of the year are represented by a circle ($2\pi = 6.28$ rad). The angle θ_m denotes the position of the mid-day of each month within the year circle (e.g., January 0.267 rad; February 0.775 rad; March 1.282 rad, etc.). Then, these vectors are summed following:

$$MSI\ (\%) = \frac{\sqrt{\left(\sum_{m=1}^{12} P_m\, sin(\theta_m)\right)^2 + \left(\sum_{m=1}^{12} P_m cos(\theta_m)\right)^2}}{\sum_{m=1}^{12} P_m} * 100 \quad (3)$$

Climate-related variables for the year of fire (2019) as well as the previous and subsequent ones were averaged to characterise the conditions before and after fire events.

Human factors have been identified as major drivers of deforestation in SSA, particularly through shifting agriculture (Curtis et al., 2018). The net rate of cropland expansion between 2003 and 2019 was derived from Potapov et al. (2022). While population density (Population, persons per km^2) was derived from Tatem (2017), the human development index (HDI), developed by the United Nations Development Programme as to measure nations' welfare, was retrieved from Kummu et al. (2018). This index ranges from 0 to 1 and could account for differences in living conditions of different regions and can be used as an indicator of population prosperity (Chuvieco et al., 2021). Finally, Gridded Livestock of the World (GLW 3) (Gilbert et al., 2018) was used to estimate the livestock density (Livestock) in Tropical Livestock Units (TLU) expressed as 250-kg-equivalent of animal units. The TLU coefficients were defined by the Food and Agriculture Organization (FAO) using a scale of 0.7 for cattle, 0.5 for buffaloes and 0.1 for goats and sheep (Bernardi et al., 2019). All climate and human datasets were aggregated to the same grid size (0.25°) by averaging.

Predictor features importance was estimated using the SHAP (Shapley Additive exPlanations) Python library (Lundberg and Lee, 2017). The feature importance values, called Shapley values, were used as a proxy to evaluate the impact of each predictor variable on the target. These values are based on the cooperative game theory (Shapley et al., 1953). The model is retrained on all feature subsets $S \subseteq F$, where F is the set of all predictor features, and then an importance value is calculated for each feature that represents a non-zero effect on the model prediction. To compute the effect of a feature i in the observation j (grid cell in our case), for each subset $S \subseteq F\backslash\{i\}$, a model $f_{S\cup\{i\}}$ including the feature i is trained, and another model f_S is trained with i withheld. The predictions from the two models are compared based on the current input $f_{S\cup\{i\}}(x_{S\cup\{i\}}) - f_S(x_S)$, where x_S refers to the values of the input features in the set S. The Shapley values are then computed. They are a weighted average of all possible differences:

$$\phi_{i,j} = \sum_{S\subseteq F\backslash\{i\}} \frac{|S|!(|F| - |S| - 1)!}{|F|!} \left[f_{S\cup\{i\}}(x_{S\cup\{i\}}) - f_S(x_S)\right]_j \quad (4)$$

where $\phi_{i,j}$ refers to the Shapley value of the feature i in the grid cell j. This method has the potential to appropriately handle multicollinearity (Lundberg and Lee, 2017) conversely to feature importance approaches used in common machine learning models such as Random Forest (Zhou et al., 2021). An example of additive Shapley values is shown in Fig. A.1.

3. Results and discussion

3.1. Overview of fire activity in SSA forests

The total BA estimated by FireCCISFD in 2019 was 4.8 Mkm^2 (4.9 Mkm^2 in 2016), out of which approximately two-thirds occurred in forest covers, that is 68 % (63 % in 2016). For the entire SSA region, the FireCCISFD BA products detected in both years significantly higher forest BA than the two coarse-resolution products: 2.08 times more than MCD64A1 and 1.66 times more than FireCCI51 in 2019. The ratios were a bit lower for 2016: 1.71 and 1.38 times more, respectively (Table 1), because of the higher omission errors for 2016: 26.5 % (Roteta et al., 2019) compared to 8.5 % in 2019 (Chuvieco et al., 2022), as the 2016 product was derived from a single S-2 satellite. The underestimation by coarse-resolution BA products was considerably more pronounced in Dry Tropical Forest (DTF), where the S-2 product detected 2.5 times more burned forest than MCD64A1, and in Moist Tropical Forest (MTF), principally in 2019 where S-2 detected 4 times more forest BA than coarse-resolution products. Such a result confirms the significant omission rates of global BA products in tropical forest fires reported by other authors (Boschetti et al., 2019; Franquesa et al., 2022). In fact, for the same year of study (2019) and using the same validation strategy, authors reported that FireCCISFD20 only omits 21.2 % of tropical forest fires, whereas MCD64A1 and FireCCI51 failed to detect 70.9 and 61.9 %, respectively (Chuvieco et al., 2022; Franquesa et al., 2022).

All BA products confirmed that Deserts & Xeric Shrublands (DXS in Table 1), which are the dominant biome of the northern Sahel as well as the Mediterranean zone of the Cape region, have marginal forest fires because of fuel scarcity and low forest cover. The DXS biome contributes to <1 % of SSA's total BA although it covers nearly a quarter of the total area (Table A.1), which can be attributed to the prevalence of unburnable barelands and very sparse fuel-limited vegetation (Fig. A.2) (Krawchuk and Moritz, 2011; Mondal and Sukumar, 2016), and where only rare and large fire events occurring during wettest years can have enough fuel to burn (Hantson et al., 2017). The Med biome, which

Table 1
Fraction of burned forest per biome over the different BA products.

Aggregated biomes	Forest area in 2019 (×1000 km^2)	Fraction of burned forest in 2019 (%)			Forest area in 2016 (×1000 km^2)	Fraction of burned forest in 2016 (%)		
		FireCCISFD	MCD64A1	FireCCI51		FireCCISFD	MCD64A1	FireCCI51
Tropical Savanna (TrS)	2922.7	46.6	23.8	30.3	2975.5	42.9	26.2	32.5
Moist Tropical Forest (MTF)	2411.6	7.3	1.8	1.8	2487.1	5.7	2.2	2.7
Dry Tropical Forest (DTF)	49.0	31.5	12.6	17.1	50.9	30.8	10.7	14.8
Temperate Savanna (TeS)	34.0	20.6	9.0	13.6	35.6	18.7	8.3	13.0
Deserts & Xeric Shrublands (DXS)	11.4	12.4	2.7	6.2	12.4	18.3	4.4	9.7
Mediterranean (Med)	11.5	3.0	2.2	2.0	12.0	5.6	3.5	3.3
SSA	5440.2	28.7	13.8	17.3	5573.5	25.9	15.1	18.8

covers a small area in the region (<0.5 % of SSA), shows low fire occurrence rates and hence contributes to a marginal proportion of the total BA across SSA (<0.15 %). Therefore, DXS and Med biomes were omitted from further analyses.

3.2. The role of fire in forest loss

The analysis of all BA products showed that fire is a major driver of land cover changes in general, and of forest loss, in particular, with a special evidence in the FireCCISFD datasets. When combining forest change for two years after burning, we estimated that on average a burned forest pixel had more than twice the chance to be converted to another land cover than an unburned pixel (2.15 times in 2019 and 2.52 in 2016), with lower proportions for the coarse-resolution BA products, particularly in Moist Tropical Forest and Temperate Savanna (Fig. 1). Fires were found to be involved in almost half of forest losses in SSA (46 ± 3.80 % in 2019 and 47 ± 4.21 % in 2016).

Depending on biomes and the year of study, fire-related forest cover loss ranged from 32 ± 1.83 % to 75 ± 3.65 % of total losses (Fig. 2). The lower values were found in MTF because of their dense canopy and high moisture, which constrain fire ignitions and limit fire spread (Krawchuk and Moritz, 2011). However, the relative impact of fire occurrence on forest losses was prominent in this biome as well (Fig. 1). In fact, in MTF the probability of a burned forest to change to another cover was up to 6 times higher than for unburned areas in 2019 and 8 times higher in 2016. It suggests that although fire activity was limited in MTF, its relative repercussions on forest cover were prominent, mainly because of the limited resistance of MTF trees to fire events (Poorter et al., 2014; Scheper et al., 2021). Most MTF tree species carry poor resistance strategies thus experiencing high mortality during fires, along with poor

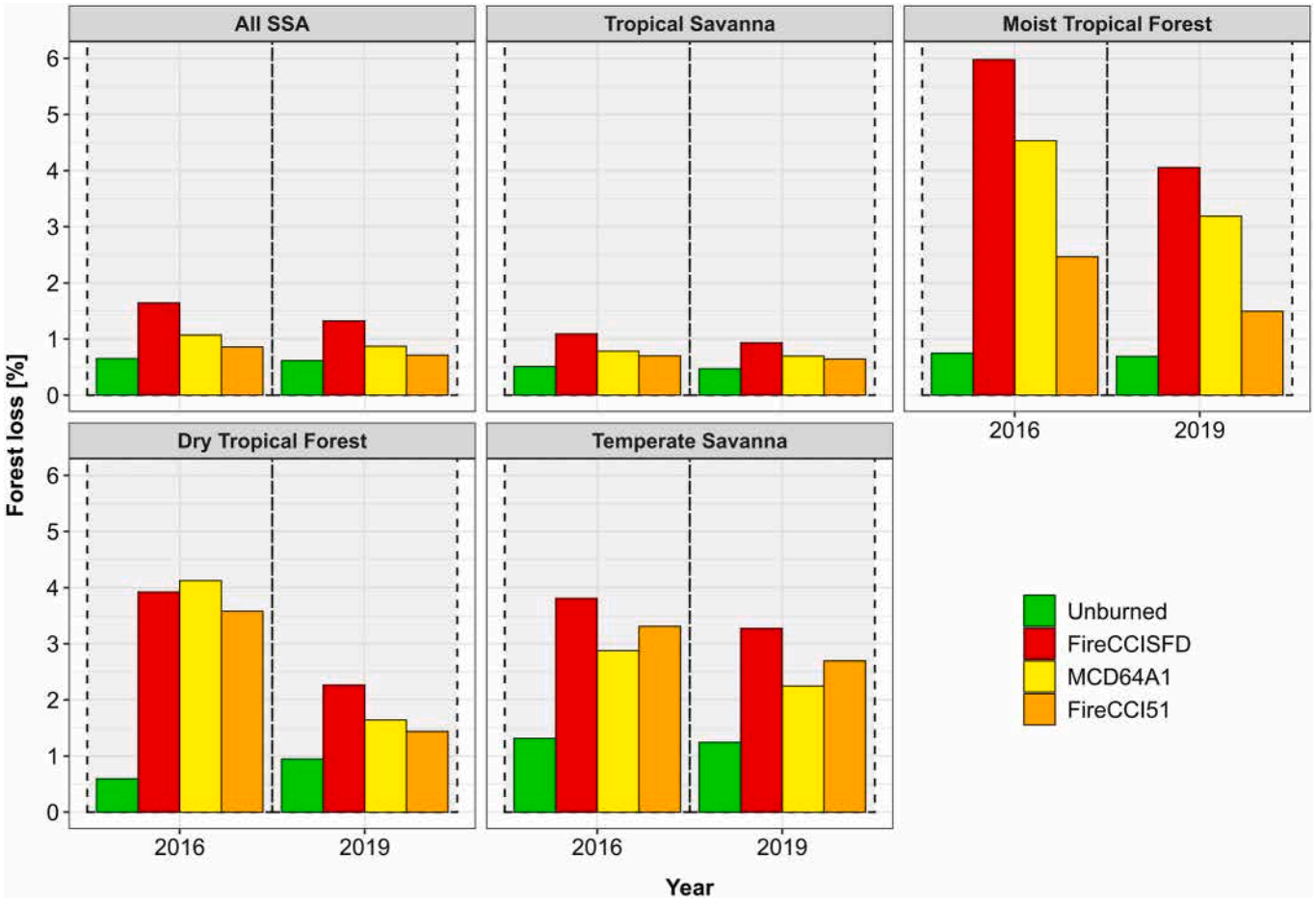

Fig. 1. Forest loss proportions in each biome attributed to unburned and burned area (for different BA products). Unburned refers to forest areas classified as not burned in the FireCCISFD product.

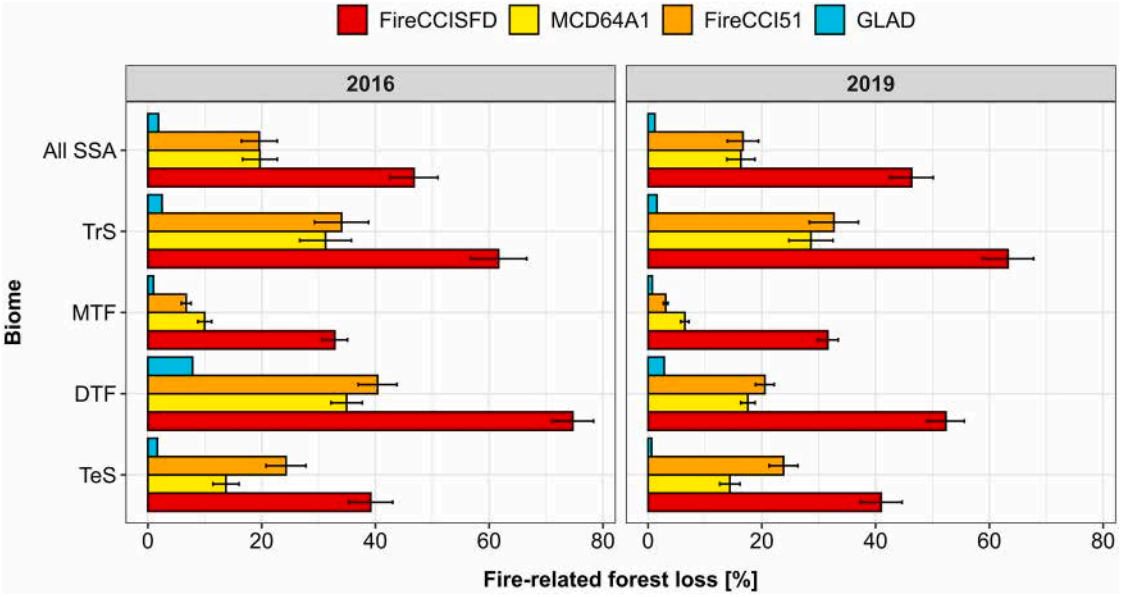

Fig. 2. Fire-related forest loss comparison between BA products. The bars refer to the average of the best estimate of fire-related loss weighted by the area of forest loss within each grid cell of 0.05°. The error bars denote the 95 % confidence interval, while for GLAD, there was no uncertainty estimate provided.

post-fire recovery, observed even after several years from burning (Ferry Slik et al., 2002; Nikonovas et al., 2020).

Similar findings were observed in dry forests (DTF), particularly during 2016 when the fraction of forest cover loss was >6 times higher in burned patches than in unburned ones. The conjunction of the high probability of forest fires to be followed by loss and the high level of fire occurrence in 2016 resulted in a fire contribution to forest losses reaching 75 %, significantly higher than in 2019 (52 ± 3.24 %). The extreme drought conditions prompted by the 2015–2016 El Niño Southern Oscillation event are likely to be the main driver of the larger loss of DTF from fires, since those water-limited forest ecosystems are very sensitive to the interannual weather variability (Ahlstrom et al., 2015).

In tropical savannas (TrS) tree species are well adapted to fires and therefore the subsequent losses were lower compared to other biomes (only ~1 % in 2016 and 2019). Fire-adapted tree species of savanna ecosystems are avoidant (self-pruning or elevated canopy base height preventing surface fires to extend to the canopy) and resistant to fire, through specific life-history strategies and functional traits (Bond et al., 2005; Pausas, 2019; Pausas et al., 2004). These species also present efficient resilience traits thanks to their greater allocation to coarse roots and their plastic responses to light in comparison with other forest species (Hoffmann and Franco, 2003; Hoffmann et al., 2003). These strategies involve sprouting and allow seedlings to survive next fires (Bond et al., 2005). Moreover, fire and herbivory interactions constitute another mechanism that facilitates tree recovery in TrS. High levels of grazing reduce grass fuel load, which is later reflected in a lower flammability and intensity of fires, with lower tree damage and a higher competitive advantage for trees to acquire resources (Van Langevelde et al., 2003). These mechanisms reduce the impacts of fire on TrS tree cover loss. Nevertheless, due to the frequent and intense burning regimes within this biome, fire remains the major source of tree disturbances and drives >60 % of forest loss. In temperate savannas (TeS) the abundance of temperate highland C_3 grass species is generally altering fire spread and activity, yet in the north-eastern zone of the Highveld grasslands associated with important tree cover proportions, exceptional fire activity was observed, which highly contributed to forest losses (Fig. A.3). It is worthwhile to mention that the threshold used for forest cover fraction (30 %) excludes sparse trees in savannas (both TrS and TeS), which is probably the main reason for the relatively high uncertainties in TrS.

On average, S-2 BA products give more than twice larger fire-related forest loss than the coarse-resolution products. Substantial differences were found in MTF, especially in 2019 where MCD64A1 and FireCCI51 failed to estimate a significant proportion of BA (Table 1) and gave 5 and 10 times less fire-related loss than S-2, respectively. This might also suggest that the lower omission errors of the 2019 version of FireCCISFD provided an enhanced potential to capture an additional proportion of small fires leading to forest damages within humid ecosystems. Significant differences were also noticed in the rates of forest loss fractions within burned regions detected using the different products (Fig. 1). These differences are mainly linked to the commission errors of coarse-resolution products, which engender an interference of actually unburned areas generally implying smaller fractions of forest loss. Additionally, the omission of small-scale fragmented burns used to clear forests lowers the estimations of the contribution of fire to forest loss in coarse-resolution datasets, which aligns with the fact that >60 % of small fires (<125 ha, in this reference) detected by S-2 BA in 2019 were missed by coarse-resolution products (Chuvieco et al., 2022).

The comparison with the GLAD product (30 m) (Tyukavina et al., 2022) revealed an underestimation of forest loss due to fires, 45 % less than our S-2 based estimations and 15 % smaller than the coarse-resolution BA products. The main reason of this discrepancy is linked to the more restrictive GLAD definition of fire as a driver of forest loss, based on a classification model of forest loss drivers where fire attribution includes only wildfires not followed by agricultural activities (Tyukavina et al., 2018; Tyukavina et al., 2022). Therefore, using such an approach it was reported that shifting agriculture accounts for 92 % of forest losses in Africa, while wildfires drive no more than 1 % of these losses (Curtis et al., 2018). In reality, fire is strongly associated with shifting cultivation through slash-and-burn practices (Davidson et al., 2008), but Earth observation sensors cannot accurately distinguish whether fire initiates or follows deforestation practices, given the short time intervals in which these events occur (typically 1–2 months). Moreover, burned lands (also called swiddens), particularly over fertile soils, are exposed to a decline of soil carbon and nitrogen with limited recovery over time (Pellegrini et al., 2018).

To assess the short-term fate of fire-induced tree cover loss, NDVI change before and after fire has been evaluated as a proxy of forest productivity (Gazol et al., 2018). A notable decrease of this vegetation

index was constantly observed in all biomes in areas affected by forest losses, especially in DTF, where the drop reached 25 %. On the other hand, burned forests that were capable to resist fire events didn't show a significant NDVI drop (Fig. A.4). Such a decline in forest productivity confirms the adequacy of GFC to assess the fate of tree covered areas following fire disturbance.

3.3. Forest loss and fire impacts at country level

An estimated gross area of 36,690 km^2 of SSA's forest cover was lost during the year 2019, compared to 41,170 km^2 in the dry year of 2016. In general, the equatorial belt (5° N to 5° S), characterized by the prevalence of MTF, had lower fire-related forest losses, whereas in TrS and DTF, fire was the dominant driver associated with forest loss (Fig. 3B and D).

At a country level, the Democratic Republic of the Congo (DRC) accounted for approximately one-third of total forest area losses in 2019 and 2016, of which 44 and 38 % were fire-related, respectively (Fig. 4). This rate was noticeably high in the tropical savanna of DRC (Extended Data Tables A.2 and A.3) as well as in Zambia, Mozambique and Angola, where TrS is dominant. Forest losses in the aforementioned countries were associated with the largest expansion of croplands during the last two decades (Potapov et al., 2022), which indicates a widespread utilisation of slash-and-burn farming (Kalaba et al., 2013; Montfort et al., 2021).

Among countries with high losses (>1000 km^2), the severe drought of the 2015–2016 El Niño Southern Oscillation resulted in higher forest losses in 2016 than in 2019 in most of them, except in countries highly dominated by MTF (i.e. Ivory Coast, Liberia and Cameron). This finding is in accordance with the drought-resistance plant strategy found within these ecosystems during extreme climate anomalies (Bennett et al., 2021). The case of Madagascar needed further investigations as the losses in 2016 were 50 % higher than in 2019. These losses were also associated with a large contribution of fires, reaching up to 48 % in 2016

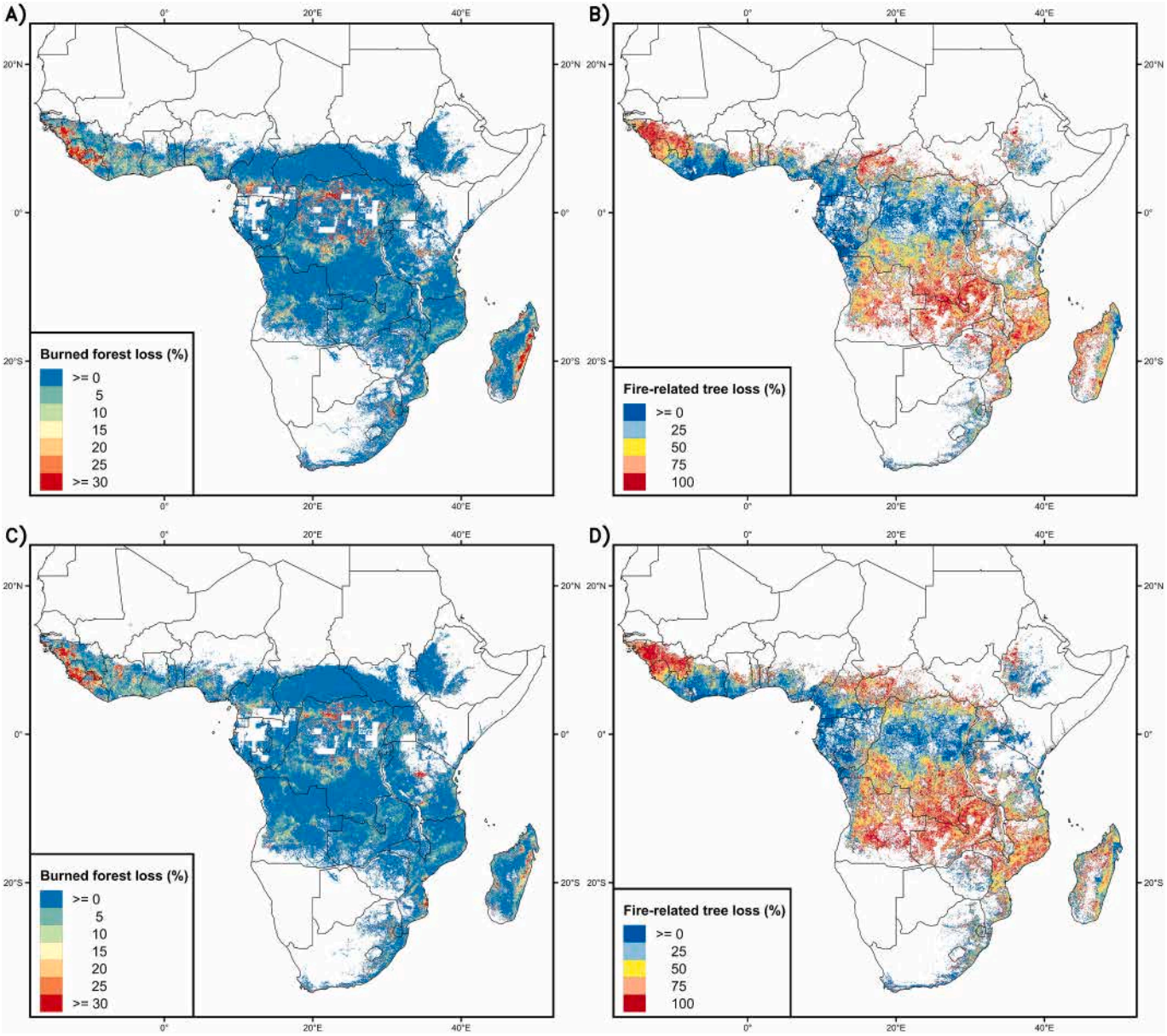

Fig. 3. Fire impact on forest loss from FireCCISFD calculated through two parameters: the fraction of tree cover loss within burned forests in 2016 (A) and 2019 (C), and fire-related forest loss for the same years 2016 (B) and 2019 (D). The former indicates the percentage of burned area that was deforested, while the latter shows what proportion of total deforested area was fire-related.

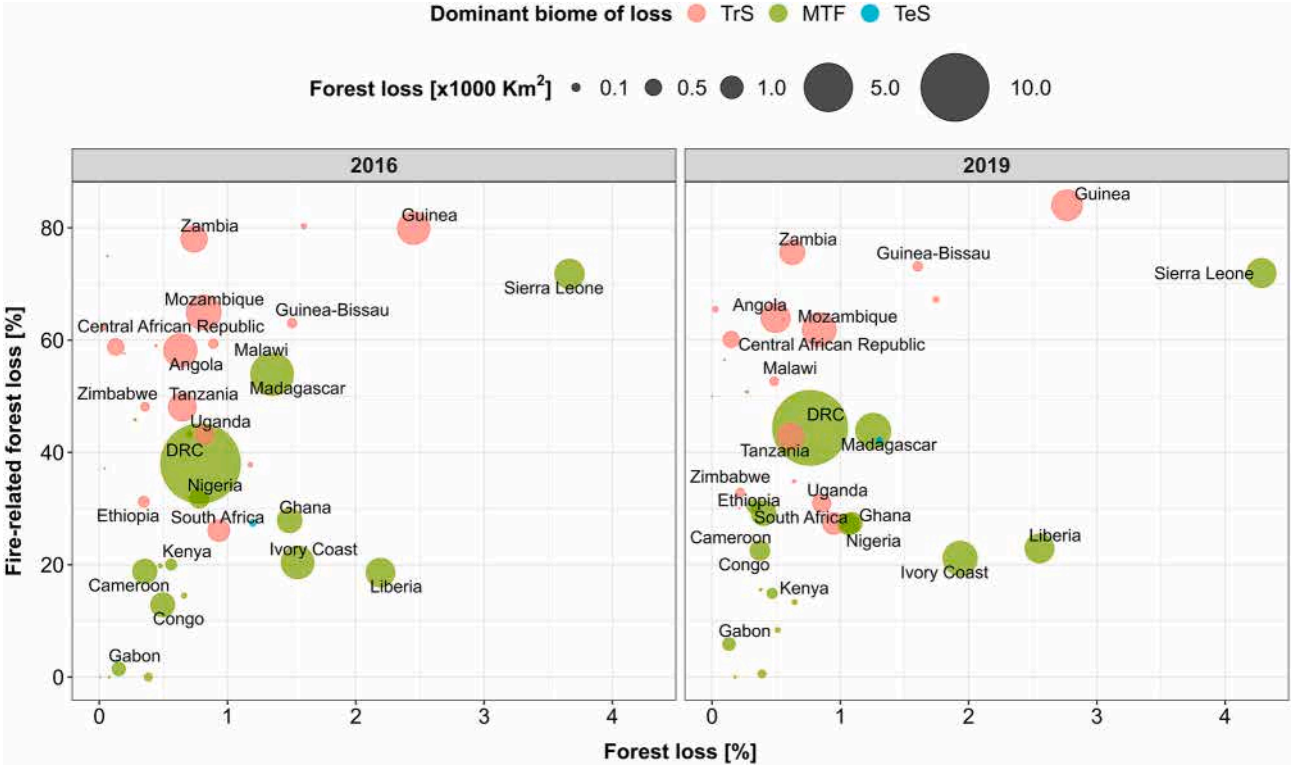

Fig. 4. Fire-related forest loss (in proportion to total forest loss) vs total forest loss (in proportion to total forested area) across countries of SSA in 2016 and 2019. Countries with forest losses lower than 100 km^2 were not labelled. Colour of circles indicates the most affected biome by fire-related deforestation (see Table A.2).

(Table A.2) even in the MTF zone. These losses are mainly attributed to pastureland management practices using fire to stimulate the encroachment grass appreciated by cattle instead of woody plants presenting unpalatable lignified stems and to maintain certain vegetation types commonly used for subsistence foraging (Bloesch, 1999). On the other hand, several authors confirmed a drastic forest stand-replacement experienced in west SSA during the twentieth century (Fairhead and Leach, 1998; Rudel et al., 2009; Sayer et al., 1992). This process was mainly driven by cropland expansion and is still largely pronounced (Fig. 3A and C), especially in drier ecosystems (Brandt et al., 2018; Rudel, 2013). Our analysis highlights the three distinct regimes in the region (Fig. A.5): 1) the tropical savanna regime, represented by Guinea and Guinea-Bissau, which shows broad forest losses largely associated with the occurrence of fires (55 and 47 % in 2019 and 2016, respectively); 2) the humid tropical forest regime where fires were less involved in forest loss despite the high rates of deforestation. Ivory Coast and Liberia are the major illustrative examples of this regime; 3) the Sierra Leonean case, which reveals a very particular pattern. This country represents the highest rate of forest loss (~4 % annually) and notwithstanding the fact that MTF losses were dominant (~70 %), forest fires were extensively involved in this change. This suggests that this country might be susceptible to a rapid expansion of the northwest SSA's savanna through humid forests leading to the encroachment of vegetation dominated by grasses and subject to annual fires (Leach and Fairhead, 2000). The Sierra Leonean zone revealed the most significant differences between S-2 and coarse-resolution BA products in terms of forest loss fractions associated with the presence of fires (Fig. A.6), whereas high underestimations of fire-related losses reported by the global products were also identified across the majority of dry ecosystems as well as the rainforest of eastern Madagascar (Fig. 5).

3.4. Drivers of forest loss after fire

Forest loss after fire events was linked to fire characteristics, forest structure, climate and human predictors based on an Extreme Gradient Boosting regression model (R^2 = 0.67, RMSE = 3.61 %). The model indicates that fire characteristics are highly linked to the likelihood of forest loss. More specifically, the Beta value, used as a proxy to account for the prevalence of small fires, was found to have the highest proportion of fire-related forest loss. The positive correlation of the Beta index with forest loss (Fig. 6) suggests that areas predominated by small fire patches are associated with a higher rate of fire-driven tree cover loss, in agreement with previous findings reporting the role of fire in forest conversion to fragmented small-scale agriculture (Doggart et al., 2020), which represent the major fate of deforested areas in SSA (Curtis et al., 2018; Tyukavina et al., 2018).

The association of small fires with shifting agriculture was confirmed by the positive correlation between the net cropland expansion within the period 2003–2019 (Crop-gain) and Beta (R = 0.14, p-value < 0.0001). This supports that slash-and-burn agriculture is deemed to remain driving deforestation over areas with high rates of cropland expansion during the last two decades. Fire seasonal date also had a major impact on the fate of forest cover. Fires occurring outside of the dry season, and particularly after it, tend to be a direct driver of forest stand-replacement in agreement with the findings of Krylov et al. (2014) who found that the majority of stand-replacement fires occur in late summer. The end of the fire season actually corresponds to the prevailing occurrence of more intense fire events when compared to the early fire season in northern hemisphere Africa (Laurent et al., 2019), and thus affecting individual trees with more damages. Smaller proportions of trees survived burning events occurring outside the fire season, especially in MTF and DTF (Fig. 7A). This observation was valid for all BA products; nevertheless, FireCCISFD detected more late fires than coarse-resolution products. These late fires are more frequently leading to tree damage than those within the fire season, and therefore the date of fire occurrence should be considered an important driver of fire-related deforestation over all biomes. The total forest burned area was higher in fire-adapted ecosystems such as TrS, and therefore was

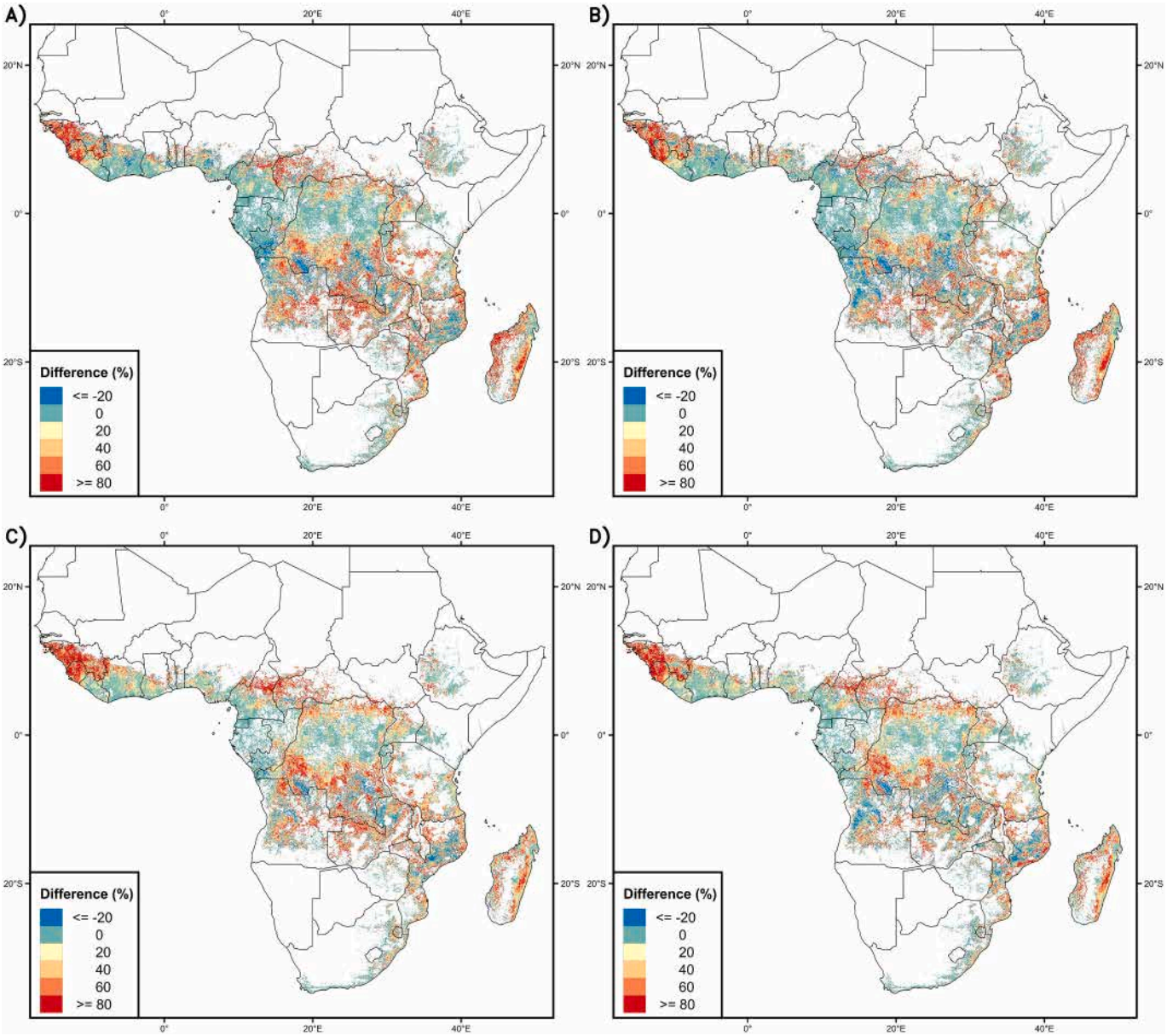

Fig. 5. Differences of fire-related forest loss estimations: (A) FireCCISFD – MCD64A1 (2016); (B) FireCCISFD – FireCCI51 (2016); (C) FireCCISFD – MCD64A1 (2019); (D) FireCCISFD – FireCCI51 (2019).

associated with lower rates of forest loss. Fire intensity was another fire parameter driving forest losses. Actually, burn events with fire radiative power (FRP) higher than 1 MW·ha^{-1} predominantly associated with forest losses (Fig. 7B).

In addition to fire characteristics, forest structure variables had a major impact on forest loss, especially in MTF (Fig. 7D). Over the entire SSA, the analysis based on distances to forest edges revealed that interior intact forests had a tendency to be less affected by fire-induced forest loss, which might be the consequence of a constrained fire spread (Cochrane et al., 1999). On the contrary, when fires occurred nearby forest edges, implicitly more fragmented, deforestation was more likely to take place. Canopy cover on edge forests is usually less dense (Ordway and Asner, 2020), so light penetration through the fragmented canopy to the ground (Nascimento and Laurance, 2002) is facilitated, which increases the dryness of the litter (Flores and Staal, 2022; Holdsworth and Uhl, 1997), and can make fires more intense and more damageable to trees (Armenteras et al., 2013; Cochrane et al., 1999). Actually, we found that fires occurring far from forest edge generally exhibit a low fire radiative power (FRP) (<1 MW·ha^{-1}) and subsequently small proportions of forest loss, while 97.5 % of the lost tree covers after fires lay within 260 m from forest edges (Fig. 7B and C). Conversely, the Above-Ground Biomass (AGB) (Santoro and Cartus, 2021) impact was influenced by the interaction with Beta (Fig. A.7A). Forest covers with medium to large AGB levels (100–200 Mg·ha^{-1}) associated with a larger number of small fires tend to be prone to fire-related loss in MTF, which could perhaps indicate a higher exposure of productive forests to conversion processes. AGB stocks larger than 200 Mg ha^{-1} didn't show a significant impact.

Climate factors (Abatzoglou et al., 2018) had a nonlinear relationship with forest loss. For instance, the high tree cover losses in moist forests of western Sahel and eastern Madagascar were mainly observed along higher rainfall gradients confirming the consistent link between deforestation and Mesoscale Convective Systems (MCSs) over tropical regions with extreme rainfall (Taylor et al., 2022), while the relatively high losses in Highveld grasslands of south-western Africa (TeS) were associated with low temperatures constraint limiting tree cover

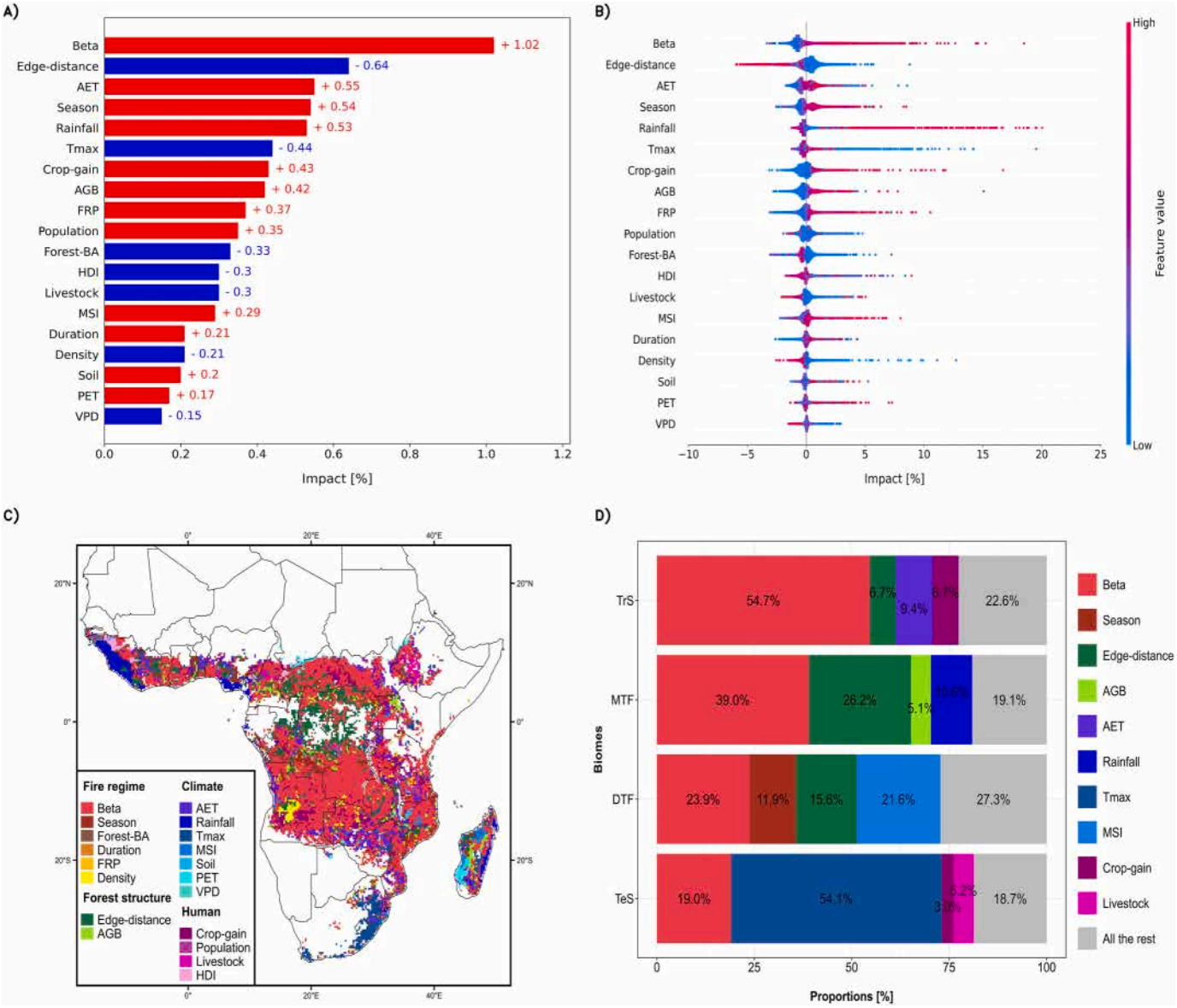

Fig. 6. Importance of drivers of forest loss after fire in 2019. (A) The mean of absolute values of impact of each predictive variable on forest loss. The sign in association with the colour indicates the direction of impact based on the correlation with the predictions (red positive, blue negative); (B) Distribution of the predictive variable's values according to their impact on the predicted forest loss; (C) Geographical distribution of the most important predictor variables explaining forest loss per grid cell; (D) Proportions of the most important predictor variables explaining forest loss per biome. The impact values are derived from the Shapely feature importance analysis of the XGBoost model.

regrowth in such high-altitude ecosystems (Lehmann et al., 2011). The Actual Evapotranspiration (AET) was strongly positively correlated with rainfall ($R = 0.74$, p-value < 0.0001) and both parameters were linked with large forest losses at extreme ranges, especially the latter one (Fig. A.7B and C). Population density (Tatem, 2017) showed a low impact on forest losses and had an apparent positive impact only at low-density ranges (<50 persons per km^2, see Fig. A.7D and E), which characterise rural populations (Tritsch and Le Tourneau, 2016). It might evidence the high pressure exerted by dense rural communities far from urban centres on forest ecosystems. The rest of human indicators didn't exhibit remarkable influence.

The study evidences the potential of medium-resolution BA datasets such FireCCISFD and GFC to enhance our understanding of fire impacts on forest loss over coarse-resolution products, particularly, in tropical regions dominated by small fires. Nevertheless, some limitations should be acknowledged. Notably, due to the tremendous computational resources involved in the product generation, the FireCCISFD datasets only cover two years (2016 and 2019), hindering a comprehensive long-term assessment of fire history and impacts. Furthermore, the GFC dataset keeps track of forest gains only until 2012, subsequently, the young trees were overlooked. The GFC was also found to have low sensitivity to sparse tree covers (Reiner et al., 2023). Actually, up to 30 % of additional tree cover was detected using high-resolution nano-satellites (<3 m spatial resolution), which would increase the estimation of forest loss fractions after fires as these areas are highly fragmented (Reiner et al., 2023). Ultimately, distinguishing between shifting agriculture techniques solely reliant on fire and those involving fire along with other mechanical operations (i.e., cutting part of or the integrity of the tree before burning) using common medium-resolution data sensors is extremely challenging and therefore in all of these cases fire was considered as a driver of loss.

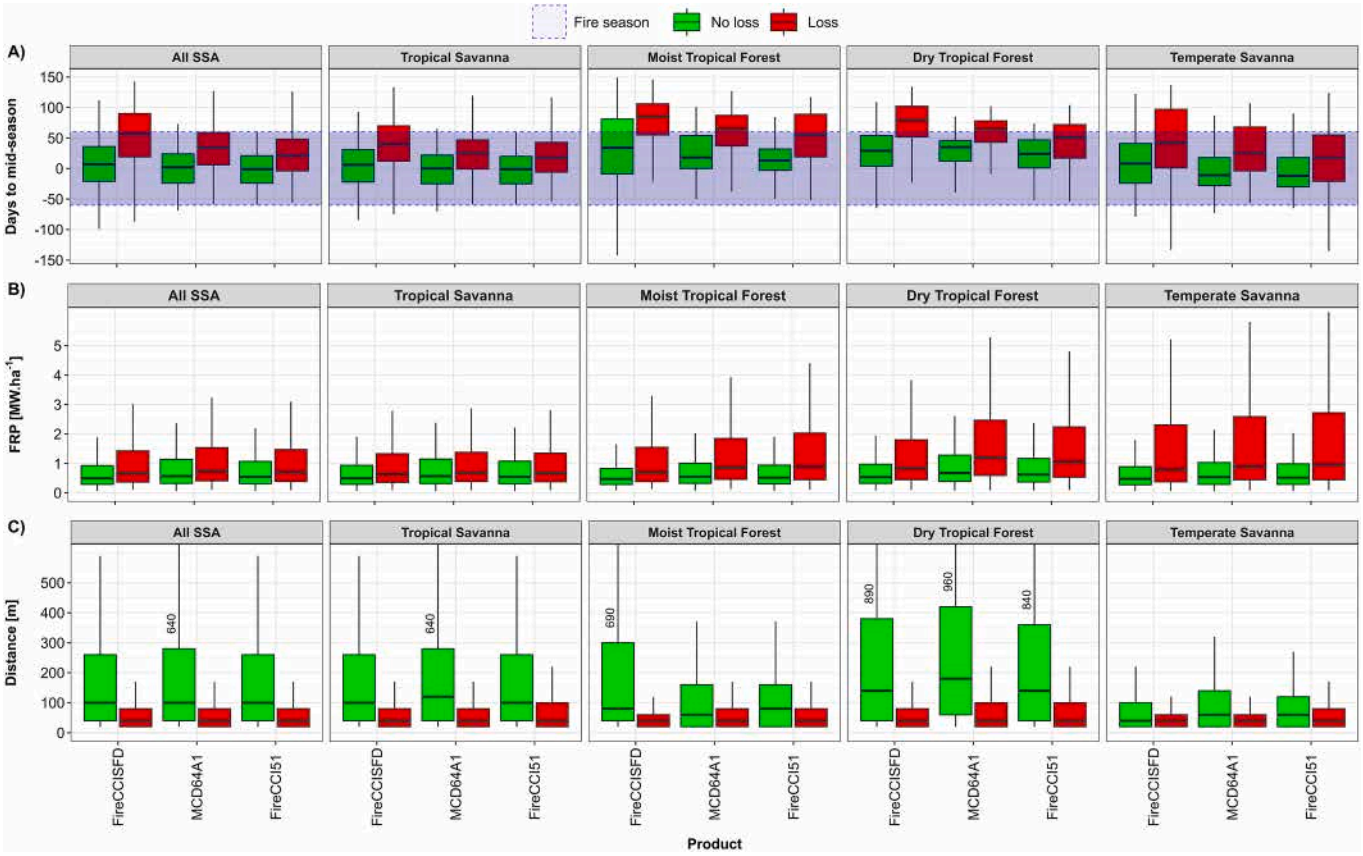

Fig. 7. Impact of fire properties on loss or no loss of burned forests in 2019. (A) BD difference with the mid-fire season in days; The blue horizontal band represents the four months of fire season; (B) Intensity of fires estimated through FRP; (C) Distance to forest edge. In the case where the 1.5 interquartile range, in either direction of boxplots, is farther from the median (absolute difference) than the limits of the 95 % confidence interval, the values of this later are retained in boxplot whiskers. The numbers above boxplots indicate the value of whiskers falling outside the y-axis limit.

4. Conclusions

This study presented different perspectives to compare medium- and coarse-resolution BA products over SSA, the most burnable region worldwide. The emphasis was dedicated to the assessment of fire impacts on forest loss and degradation. The discrepancies in estimations derived from both resolution products were significant but varied depending on biomes and the particular characteristics of regions. In any case, our study reveals that the quantification and the understanding of the relationship between fires and tropical deforestation need to be based on higher spatial-resolution BA datasets ($\leq$30 m) rather than those currently used, which are based on coarse-resolution sensors. The substantial omissions of small fires used to clear forests for various purposes, ranging from shifting agriculture to pastureland management to industrial commodities, remain the main reason that might explain the differences found in this paper between medium and coarse-resolution data estimations. We found that MTF biome was extremely vulnerable to fire events, and that global BA products noticeably underrepresent the impacts of fire on this ecosystem. The interannual comparison of forest loss responses to extreme drought caused by anomalous climate events such as the 2015–2016 El Niño Southern Oscillation event revealed positive feedback (i.e. an increase of loss) in dry forest ecosystems and an important resistance of moist rainforest. However, the impact of fire has significantly exacerbated forest loss, especially in Madagascar, in which we found higher fire-related forest stand-replacement not only in DTF but also in the tropical rainforest (MTF). The review of policy-making strategies with regard to forest conservation is highly encouraged and must be prioritized in parallel to the socio-economic strategies to attain consistent and sustainable development goals. Similar recommendations can be raised about the situation of the Democratic Republic of the Congo, Zambia, Mozambique, Angola and western countries of the Sahel, particularly Sierra Leone, which seems to present a massive expansion of savanna fire regimes over moist forest ecosystems. Fire size distribution, as measured by the Beta coefficient, confirm the dominant role of small fires, generally associated with slash-and-burn agriculture in deforestation across the SSA, while the analysis of fire season and intensity, as well as forest density, complements our understanding of the impact of fires on forest ecosystems. In fact, fires occurring towards forest edges, which are associated with intense fire flames, as well as late-season fires had higher probabilities of forest loss. With that regard, S-2 allowed better detection of less intense fires towards the late season and fragmented forest edge than coarse-resolution products. The assessment of long-term tree cover fate along with fire occurrence using medium-resolution datasets would present a great potential to generalise the results of this study and evaluate particular trends and patterns. Moreover, it would allow to disentangle forest losses solely triggered by fires from losses involving the use of other drivers prior to burning such as mechanical clearing and felling widely used in slash-and-burn conversions.

CRediT authorship contribution statement

Amin Khairoun: Writing – review & editing, Writing – original draft, Visualization, Validation, Software, Methodology, Investigation, Formal analysis, Data curation, Conceptualization. **Florent Mouillot:** Writing – review & editing, Supervision, Methodology, Formal analysis, Conceptualization. **Wentao Chen:** Software, Resources, Methodology.

Philippe Ciais: Writing – review & editing, Writing – original draft, Supervision, Conceptualization. **Emilio Chuvieco:** Writing – review & editing, Writing – original draft, Validation, Supervision, Methodology, Investigation, Funding acquisition, Conceptualization.

Declaration of competing interest

The authors declare that they have no known competing financial interests or personal relationships that could have appeared to influence the work reported in this paper.

Data availability

Data will be made available on request.

Acknowledgements

The FireCCISFD20 product was generated under the FireCCI project (https://climate.esa.int/en/projects/fire/, last consulted October 2023), which is part of the European Space Agency's Climate Change Initiative (ESA CCI) programme (Contract No. 4000126706/19/I-NB). We would like to thank Mihai Tanase for his technical support. We would also like to thank Dave van Wees and Ekhi Roteta for sharing their datasets.

Appendix A

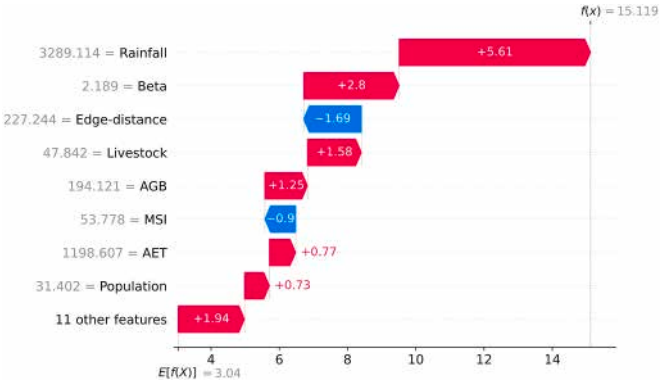

Fig. A.1. Example of additive Shapely values explaining the predictions of forest loss. The grid cell was located in Ghana (MTF). The predicted forest loss value (f(x) = 15.119 %) was significantly higher than the mean (E[f(X)] = 3.04 %). Rainfall and Beta had higher values than their respective means and contributed to the increase of forest loss by 5.61 and 2.8 %, respectively (positive correlation), while Edge-distance that is negatively correlated with the target, was leading the rate of forest loss to decrease by 1.69 %. Without the latter variable, the model expects to estimate a forest loss rate of 16.809 %.

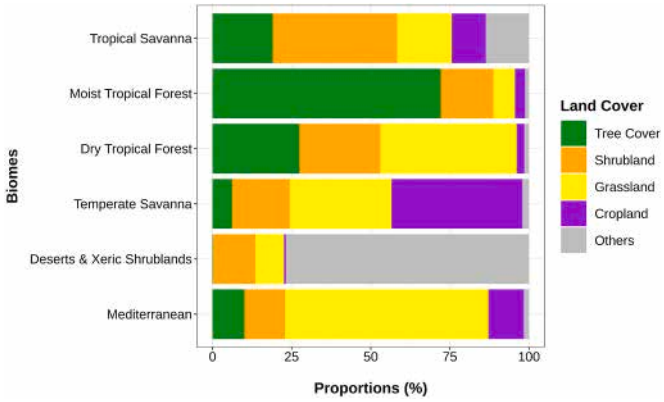

Fig. A.2. Proportions of land cover types per biome in 2019.

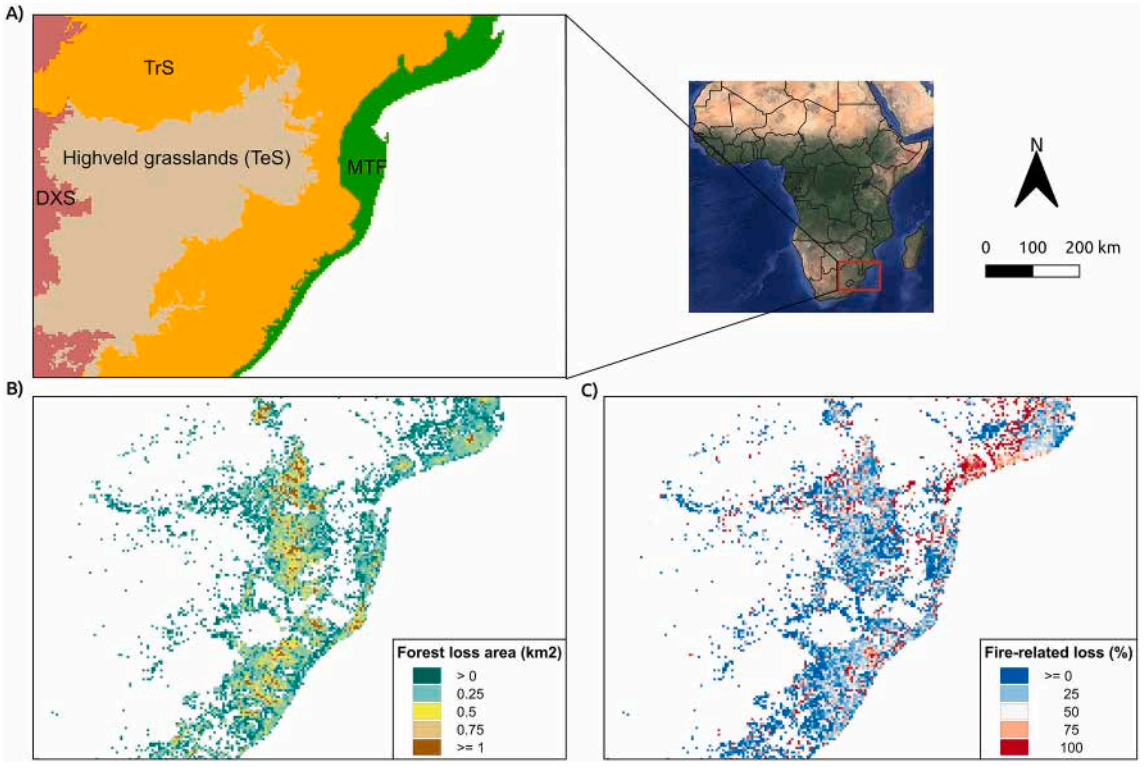

Fig. A.3. Impact of fire on Temperate Savanna trees in 2016. (A) Biomes; (B) Area of forest loss; (C) Fire-related loss.

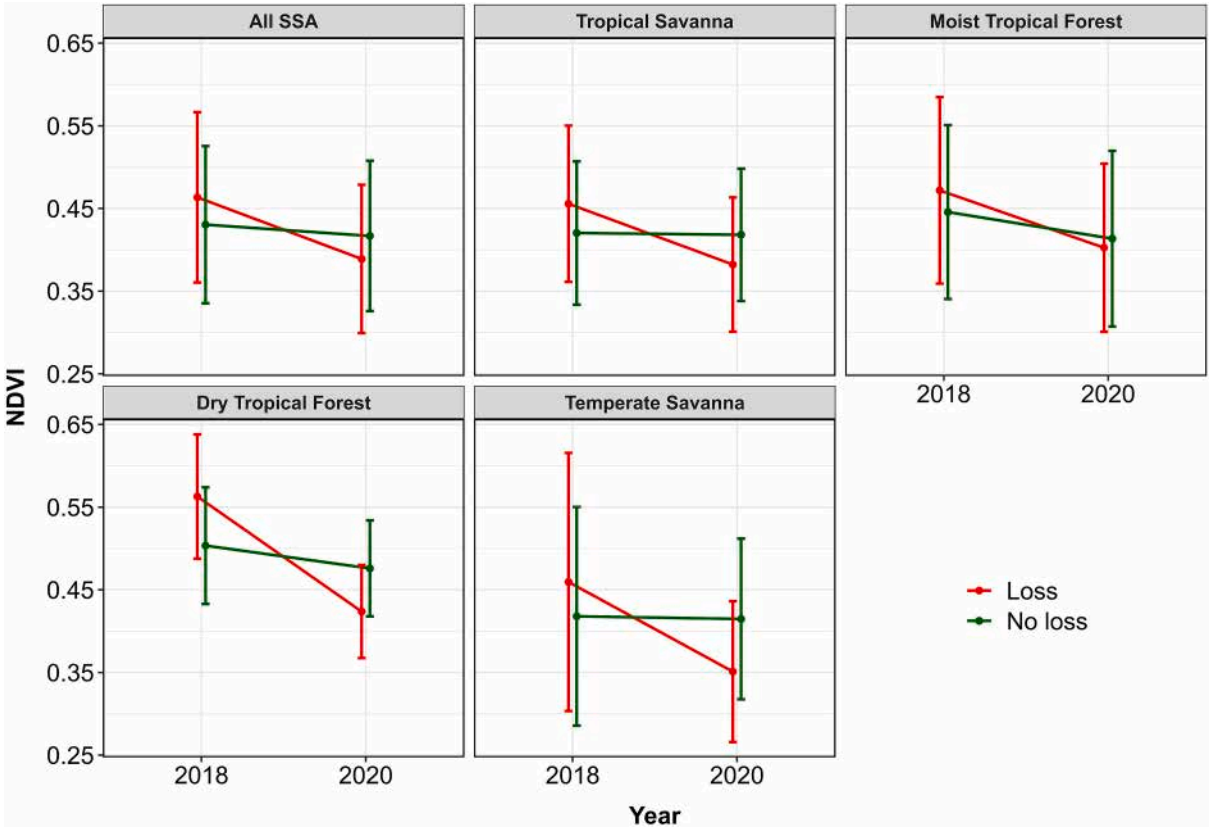

Fig. A.4. NDVI change between before and after fire year (2019). The dots represent the biome mean of annual composite medians. The error bars denote the standard deviation.

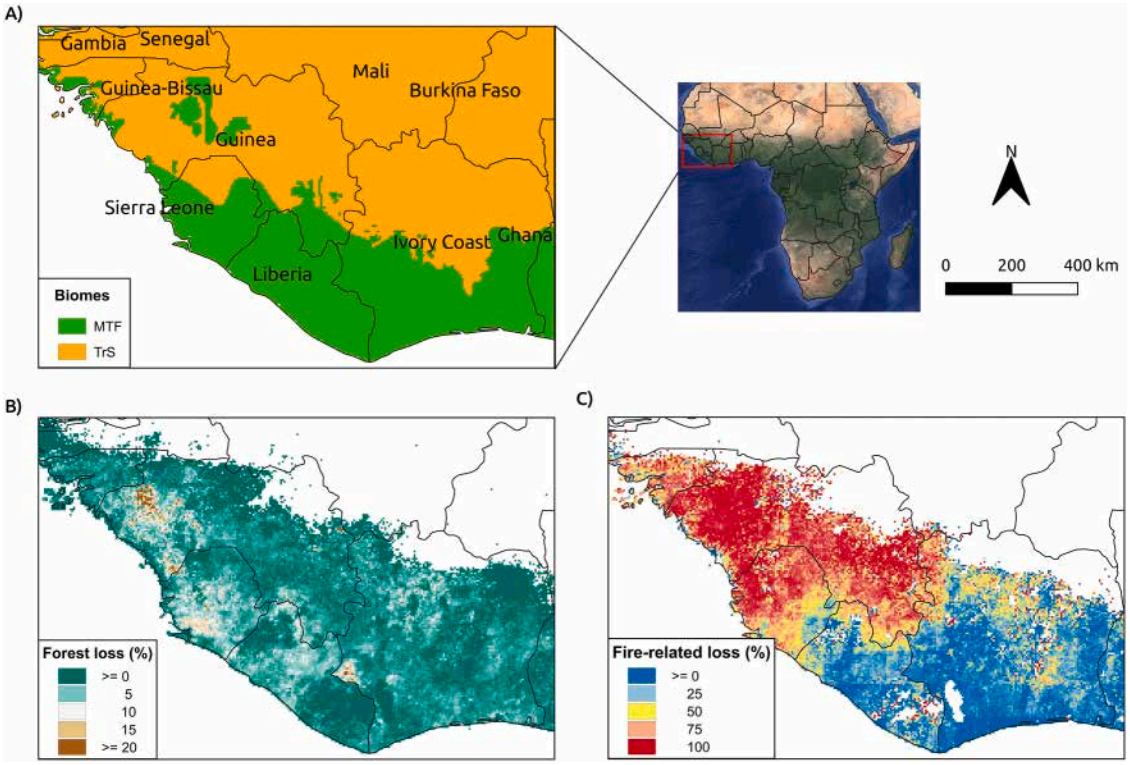

Fig. A.5. West SSA's regimes. (A) Biomes and countries; (B) Forest loss fraction; (C) Fire-related forest loss. The maps were based on data of 2019.

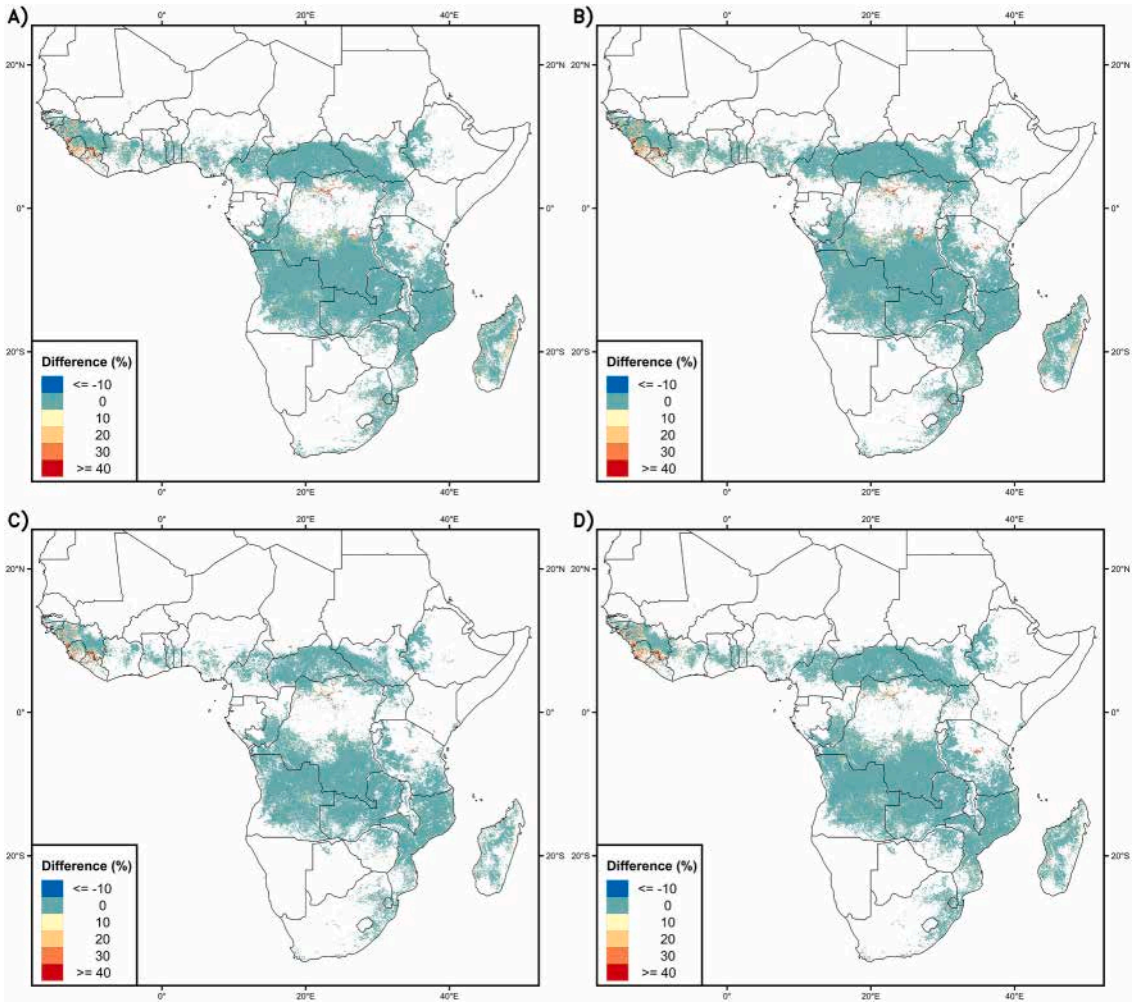

Fig. A.6. Differences of estimations of the fraction of tree cover loss within burned forests: (A) FireCCISFD – MCD64A1 (2016); (B) FireCCISFD – FireCCI51 (2016); (C) FireCCISFD – MCD64A1 (2019); (D) FireCCISFD – FireCCI51 (2019).

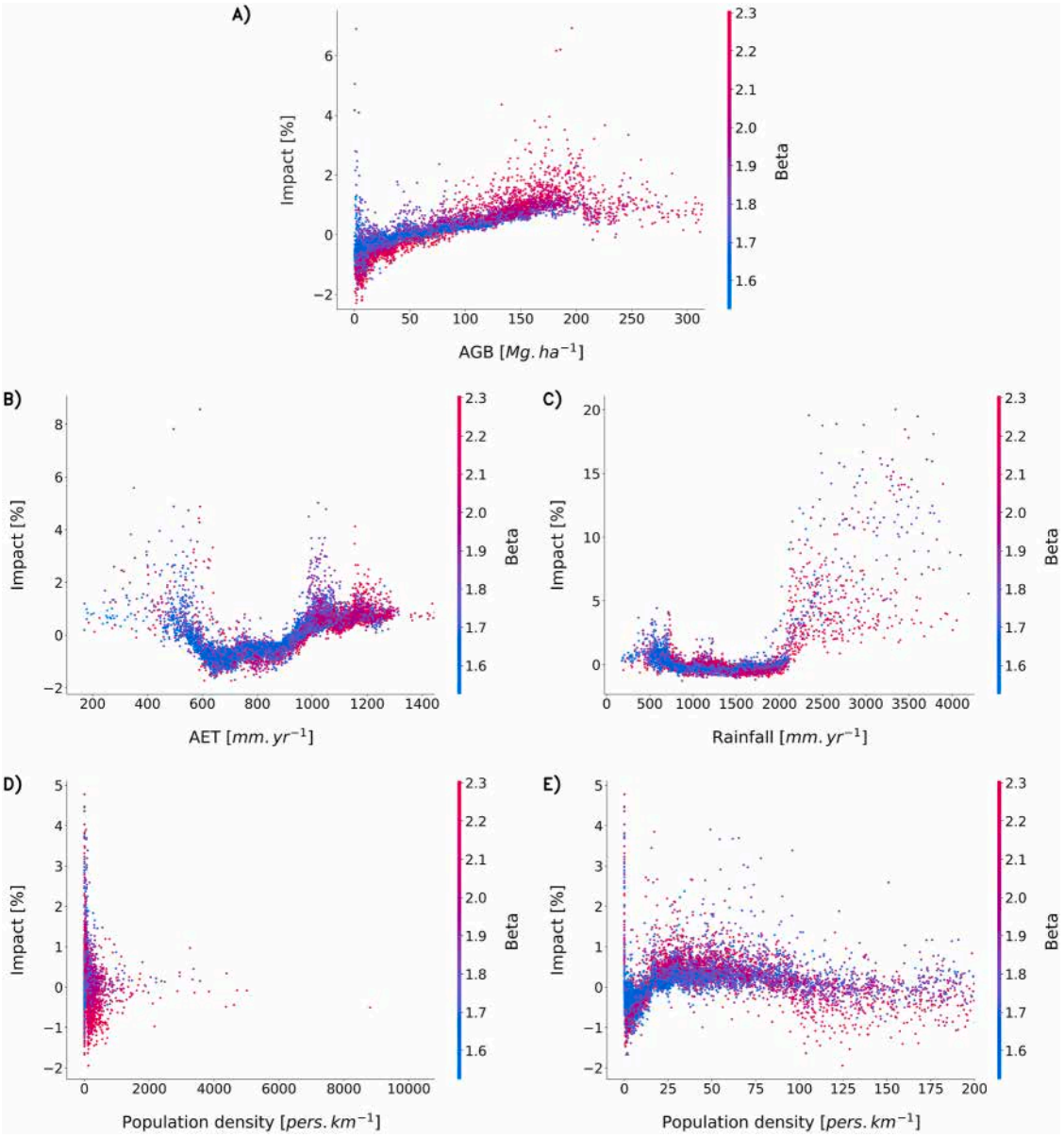

Fig. A.7. Partial dependence plots of some predictor variables with their impact on forest loss predictions. (A) AGB; (B) AET; (C) Rainfall; (D) Population with the 99.99 percentile of values as an x-axis limit; (E) Population filtered with a maximum of 200 persons per km^2. Except for E, all the other plots were limited to the 99.99 percentile along the x-axis. The colour indicates the interaction with Beta, the most dominant variable explaining forest loss predictions.

Table A.1
Reclassification scheme of terrestrial biomes.

Aggregated biomes	Original Dinerstein's ecoregions	Proportion of SSA (%)	Proportion of SSA BA (%)	
			2019	2016
Tropical Savanna (TrS)	Tropical & Subtropical Grasslands, Savannas & Shrublands Flooded Grasslands & Savannas (latitude 23° S to 23° N)	60.62	88.49	88.71
Moist Tropical Forest (MTF)	Mangroves Tropical & Subtropical Moist Broadleaf Forests	13.23	8.23	7.39
Dry Tropical Forest (DTF)	Tropical & Subtropical Dry Broadleaf Forests	0.71	1.42	1.61
Temperate Savanna (TeS)	Montane Grasslands & Shrublands Flooded Grasslands & Savannas (latitude >23° S or 23° N)	2.13	1.04	1.08
Deserts & Xeric Shrublands (DXS)	Deserts & Xeric Shrublands	22.82	0.78	1.06
Mediterranean (Med)	Mediterranean Forests, Woodlands & Scrub	0.46	0.04	0.15

Table A.2
FireCCISFD estimations of fire-related forest loss across SSA countries in 2016. Fire-related forest loss is estimated within biomes of each country (columns 2–5). Columns 7–10 indicate the contributions of the different biomes to the total forest losses by country. The biome with the highest contribution is used in Fig. 4.

Country	Fire-related loss (%)					Distribution of forest losses by Biome (%)				Forest loss (Km^2)
	DTF	MTF	TeS	TrS	Average	DTF	MTF	TeS	TrS	
DRC		17.12	4.73	55.54	38.04		61.45	~ 0	38.55	13847.14
Madagascar	63.72	47.72	41.71		53.92	11.77	88.05	0.18		3843.9
Mozambique		60.56	62.99	66.92	64.93		33.49	0.15	66.36	2521.42
Angola	87.35	2.75	64.57	58.3	58.18	0.14	0.59	1.79	97.48	2294.76
Ivory Coast		7.93		37.06	20.41		83.47		16.53	2219.11
Guinea		71.85		82.91	79.91		32.76		67.24	2178.55
Sierra Leone		70.7		75.08	71.78		81.01		18.99	1766.56
Liberia		18.52		47.5	18.6		99.27		0.73	1678.38
Tanzania		40.6	34.61	50.52	48.07		32.07	3.64	64.29	1565.24
Zambia	86.77		72.31	77.79	78.03	9.01		~ 0	90.99	1415.29
Ghana		17.18		57.51	27.89		95.21		4.79	1205.5
Cameroon		9.69		36.19	18.83		80.64		19.36	1164.86
Congo		10.29		16.42	12.87		69.39		30.61	1149.16
South Africa		30.64	29.45	24.47	26.08		13.59	32.74	53.67	940.18
Nigeria		22.61	34.88	45.9	31.83		84.91	0.01	15.08	729.24
Uganda		37.51	10.13	46.32	43.15		25.51	0.01	74.48	686.01
Central African Republic		33.82		63.72	58.8		47.64		52.36	513.95
Gabon		0.45		5.16	1.44		73.01		26.99	314.71
Kenya		17.15	20.73	24.39	20.03		83.22	0.67	16.1	201.23
Ethiopia		25.13	11.95	44.23	31.22		36.53	13.21	50.26	199.54
Malawi		4.17	62.32	59.78	59.38		0.47	23.86	75.67	139.76
Guinea-Bissau		53.95		67.06	63.04		36.64		63.36	139.09
Zimbabwe		62.49	45.04	48.23	48.14		8.86	39.82	51.32	117.93
Equatorial Guinea		0			0		100			91.4
eSwatini		56.7	24.11	27.37	27.47		0.05	60.89	39.06	62.84
South Sudan		57.51		62.52	62.22		7.01		92.99	41.99
Togo		44.83		42.69	43.24		61.09		38.91	35.68
Chad				80.29	80.29				100	30.44
Rwanda		8.82		27.77	14.51		94.31		5.69	29.37
Benin		18.33		38.24	37.81		20.41		79.59	22.5
Burundi		15.58		26.81	19.81		81.08		18.92	16.1
Mali				58.98	58.98				100	3.01
Senegal		31.89		48.39	45.81		63.2		36.8	2.44
Somalia		47.05		60.88	50.79		63.58		36.42	0.91
Comoros		0			0		100			0.87
Lesotho			4.41	0	2.98			73.01	26.99	0.29
Sudan				74.95	74.95				100	0.27
Gambia		63.72		59.66	57.6		6.49		93.51	0.06

The colours in columns 2–5 enhance the visual interpretations of fire-related loss with purple as the low (0 %) and the red as the highest (100 %). The red values in columns 7–10 indicate the biome with highest rate contribution to forest loss in each country.

Table A.3
FireCCISFD estimations of fire-related forest loss across SSA countries in 2019. The estimations are calculated in the same way as in Table A.2.

Country	Fire-related loss (%)					Distribution of forest losses by Biome (%)				Forest loss (Km^2)
	DTF	MTF	TeS	TrS	Average	DTF	MTF	TeS	TrS	
DRC		23.21	68.21	61.94	44.38		63.05	0.01	36.94	12221.87
Madagascar	47.16	43.55	22.54		43.85	19.03	70.5	0.21		2551.2
Ivory Coast		9.98		35.97	21.13		80.51		19.49	2432.26
Mozambique		54.29	40.7	64.74	61.89		38.88	0.19	60.93	2374.29
Guinea		76.62		86.73	84.01		32.88		67.12	1947.75
Angola	84.01	7.41	71.88	64.13	63.94	0.11	0.73	2.42	96.68	1745.69
Sierra Leone		67.94		83.54	71.94		85.17		14.83	1743.3
Liberia		22.83		78.95	22.91		99.58		0.42	1709.44
Tanzania		29.47	46.91	45.94	42.83		39.81	3.51	56.69	1459.28
Zambia	87.4			75.29	75.63	4.88			95.11	1247.62
Cameroon		14.33		53.91	29.2		77.34		22.66	1216.2
South Africa		27.17	32.65	30.86	27.35		13.37	29.91	56.69	930.88
Ghana		18.29		55.3	27.41		94		6	894.29
Nigeria		21.15	32.44	36.56	27.21		71.86	0.01	28.13	875.43
Congo		17.37		29.98	22.53		60.55		39.45	745.75
Uganda		28.05		32.57	30.94		21.97		78.03	644.4
Central African Republic		33.72		65.36	60.12		30.29		69.71	496.58
Gabon		2.95		16.24	5.87		79.44		20.56	279.54
Ethiopia		16.29	11.07	49.66	30.4		51.23	15.06	33.68	259.62
Kenya		14.62	28.73	14.42	14.9		79.84	0.87	19.29	168.01
Guinea-Bissau		64.17		77.17	73.14		33.19		66.81	143.71
Malawi		1.18	58.17	51.93	52.67		0.22	18.23	81.55	123.54
Zimbabwe		31.39	30.37	33.11	32.87		18.08	40.66	41.27	113.22
Equatorial Guinea		0.53			0.57		100			91.45
eSwatini		50.02	42.89	40.87	42.15		1.39	60.08	38.53	58.11
Togo		42.16		39.42	40.22		79.22		20.78	54.61
Chad				67.24	67.24				100	48.9
South Sudan		64.47		65.58	65.48		20.86		79.14	40.94
Rwanda		6.84	57.47	11.72	8.39		96.49	0.03	3.48	26.47
Burundi		13.5		13.47	13.36		75.33		24.67	24.11
Benin		38.94		34.74	34.84		1.14		98.86	9.15
Somalia		15.68		15.29	15.56		84.14		15.86	3.84
Mali				63.69	63.69				100	2.82
Senegal		56.85		49.68	50.78		63.72		36.28	2.65
Comoros		0			0		100			1.93
Sudan				56.47	56.47				100	0.56
Gambia		7.29		55.2	44.55		4.83		95.17	0.2
Lesotho			20.1	48.58	32.3			52.23	47.77	0.12

The colours in columns 2–5 enhance the visual interpretations of fire-related loss with purple as the low (0 %) and the red as the highest (100 %). The red values in columns 7–10 indicate the biome with highest rate contribution to forest loss in each country.

References

Abatzoglou, J.T., Dobrowski, S.Z., Parks, S.A., Hegewisch, K.C., 2018. TerraClimate, a high-resolution global dataset of monthly climate and climatic water balance from 1958–2015. Sci. Data 5, 170191.

Ahlstrom, A., Raupach, M.R., Schurgers, G., Smith, B., Arneth, A., Jung, M., et al., 2015. Carbon cycle. The dominant role of semi-arid ecosystems in the trend and variability of the land CO(2) sink. Science 348, 895–899.

Armenteras, D., González, T.M., Retana, J., 2013. Forest fragmentation and edge influence on fire occurrence and intensity under different management types in Amazon forests. Biol. Conserv. 159, 73–79.

Bak, P., Tang, C., Wiesenfeld, K., 1988. Self-organized criticality. Phys. Rev. A 38, 364.

Bennett, A.C., Dargie, G.C., Cuni-Sanchez, A., Tshibamba Mukendi, J., Hubau, W., Mukinzi, J.M., et al., 2021. Resistance of African tropical forests to an extreme climate anomaly. Proc. Natl. Acad. Sci. 118, e2003169118.

Bernardi, R.E., Staal, A., Xu, C., Scheffer, M., Holmgren, M., 2019. Livestock herbivory shapes fire regimes and vegetation structure across the global tropics. Ecosystems 22, 1457–1465.

Bloesch, U., 1999. Fire as a tool in the management of a savanna/dry forest reserve in Madagascar. Appl. Veg. Sci. 2, 117–124.

Bonan, G.B., 2008. Forests and climate change: Forcings, feedbacks, and the climate benefits of forests. Science 320, 1444–1449.

Bond, W.J., Woodward, F.I., Midgley, G.F., 2005. The global distribution of ecosystems in a world without fire. New Phytol. 165, 525–537.

Boschetti, L., Stehman, S.V., Roy, D.P., 2016. A stratified random sampling design in space and time for regional to global scale burned area product validation. Remote Sens. Environ. 186, 465–478.

Boschetti, L., Roy, D.P., Giglio, L., Huang, H., Zubkova, M., Humber, M.L., 2019. Global validation of the collection 6 MODIS burned area product. Remote Sens. Environ. 235, 111490.

Brandt, M., Rasmussen, K., Hiernaux, P., Herrmann, S., Tucker, C.J., Tong, X., et al., 2018. Reduction of tree cover in West African woodlands and promotion in semi-arid farmlands. Nat. Geosci. 11, 328–333.

Chen, T., Guestrin, C., 2016. XGBoost: A Scalable Tree Boosting System. Proceedings of the 22nd ACM SIGKDD International Conference on Knowledge Discovery and Data Mining. ACM.

Chuvieco, E., Pettinari, M.L., Koutsias, N., Forkel, M., Hantson, S., Turco, M., 2021. Human and climate drivers of global biomass burning variability. Sci. Total Environ. 779, 146361.

Chuvieco, E., Roteta, E., Sali, M., Stroppiana, D., Boettcher, M., Kirches, G., et al., 2022. Building a small fire database for Sub-Saharan Africa from Sentinel-2 high-resolution images. Sci. Total Environ. 845, 157139.

Clark, W.C., Tomich, T.P., Van Noordwijk, M., Guston, D., Catacutan, D., Dickson, N.M., et al., 2016. Boundary work for sustainable development: natural resource

management at the Consultative Group on International Agricultural Research (CGIAR). Proc. Natl. Acad. Sci. 113, 4615–4622.
Cochrane, M.A., Alencar, A., Schulze, M.D., Souza, C.M., Nepstad, D.C., Lefebvre, P., et al., 1999. Positive feedbacks in the fire dynamic of closed canopy tropical forests. Science 284, 1832–1835.
Curtis, P.G., Slay, C.M., Harris, N.L., Tyukavina, A., Hansen, M.C., 2018. Classifying drivers of global forest loss. Science 361, 1108–1111.
Davidson, E.A., De Abreu Sá, T.D., Reis Carvalho, C.J., De Oliveira, Figueiredo R., Kato, M.D.S.A., Kato, O.R., et al., 2008. An integrated greenhouse gas assessment of an alternative to slash-and-burn agriculture in eastern Amazonia. Glob. Chang. Biol. 14, 998–1007.
Dinerstein, E., Olson, D., Joshi, A., Vynne, C., Burgess, N.D., Wikramanayake, E., et al., 2017. An ecoregion-based approach to protecting half the terrestrial realm. Bioscience 67, 534–545.
Doggart, N., Morgan-Brown, T., Lyimo, E., Mbilinyi, B., Meshack, C.K., Sallu, S.M., et al., 2020. Agriculture is the main driver of deforestation in Tanzania. Environ. Res. Lett. 15.
Fairhead, J., Leach, M., 1998. Reframing Deforestation: Global Analyses and Local Realities: Studies in West Africa. Routledge.
Ferry Slik, J.W., Verburg, R.W., Keßler, P.J.A., 2002. Effects of fire and selective logging on the tree species composition of lowland dipterocarp forest in East Kalimantan, Indonesia. Biodiversity Conserv. 11, 85–98.
Flores, B.M., Staal, A., 2022. Feedback in tropical forests of the Anthropocene. Glob. Chang. Biol. 28, 5041–5061.
Franquesa, M., Lizundia-loiola, J., Stehman, S.V., Chuvieco, E., 2022. Using long temporal reference units to assess the spatial accuracy of global satellite-derived burned area products. Remote Sens. Environ. 269, 112823.
Gazol, A., Camarero, J.J., Vicente-Serrano, S.M., Sanchez-Salguero, R., Gutierrez, E., de Luis, M., et al., 2018. Forest resilience to drought varies across biomes. Glob. Chang. Biol. 24, 2143–2158.
Giglio, L., Boschetti, L., Roy, D.P., Humber, M.L., Justice, C.O., 2018. The collection 6 MODIS burned area mapping algorithm and product. Remote Sens. Environ. 217, 72–85.
Gilbert, M., Nicolas, G., Cinardi, G., Van Boeckel, T.P., Vanwambeke, S.O., Wint, G.R.W., et al., 2018. Global distribution data for cattle, buffaloes, horses, sheep, goats, pigs, chickens and ducks in 2010. Sci. Data 5, 180227.
Govender, N., Trollope, W.S.W., Van Wilgen, B.W., 2006. The effect of fire season, fire frequency, rainfall and management on fire intensity in savanna vegetation in South Africa. J. Appl. Ecol. 43, 748–758.
Hansen, M.C., Potapov, P.V., Moore, R., Hancher, M., Turubanova, S.A., Tyukavina, A., et al., 2013. High-resolution global maps of 21st-century forest cover change. Science 342, 850–853.
Hansen, M.C., Wang, L., Song, X.P., Tyukavina, A., Turubanova, S., Potapov, P.V., et al., 2020. The fate of tropical forest fragments. Sci. Adv. 6, 1–10.
Hantson, S., Scheffer, M., Pueyo, S., Xu, C., Lasslop, G., Van Nes, E.H., et al., 2017. Rare, intense, big fires dominate the global tropics under drier conditions. Sci. Rep. 7.
Hoffmann, W.A., Franco, A.C., 2003. Comparative growth analysis of tropical forest and savanna woody plants using phylogenetically independent contrasts. J. Ecol. 91, 475–484.
Hoffmann, W.A., Orthen, B., Nascimento, P.K.V.D., 2003. Comparative fire ecology of tropical savanna and forest trees. Funct. Ecol. 17, 720–726.
Holdsworth, A.R., Uhl, C., 1997. Fire in Amazonian selectively logged rain forest and the potential for fire reduction. Ecol. Appl. 7, 713–725.
Kalaba, F.K., Quinn, C.H., Dougill, A.J., Vinya, R., 2013. Floristic composition, species diversity and carbon storage in charcoal and agriculture fallows and management implications in Miombo woodlands of Zambia. For. Ecol. Manage. 304, 99–109.
Krawchuk, M.A., Moritz, M.A., 2011. Constraints on global fire activity vary across a resource gradient. Ecology 92, 121–132.
Krylov, A., McCarty, J.L., Potapov, P., Loboda, T., Tyukavina, A., Turubanova, S., et al., 2014. Remote sensing estimates of stand-replacement fires in Russia, 2002–2011. Environ. Res. Lett. 9, 105007.
Kummu, M., Taka, M., Guillaume, J.H.A., 2018. Gridded global datasets for gross domestic product and human development index over 1990–2015. Sci. Data 5, 180004.
Laurent, P., Mouillot, F., Yue, C., Ciais, P., Moreno, M.V., Nogueira, J.M.P., 2018. FRY, a global database of fire patch functional traits derived from space-borne burned area products. Sci. Data 5, 180132.
Laurent, P., Mouillot, F., Moreno, M.V., Yue, C., Ciais, P., 2019. Varying relationships between fire radiative power and fire size at a global scale. Biogeosciences 16, 275–288.
Leach, M., Fairhead, J., 2000. Challenging neo-Malthusian deforestation analyses in West Africa's dynamic forest landscapes. Popul. Dev. Rev. 26, 17–43.
Lehmann, C.E.R., Archibald, S.A., Hoffmann, W.A., Bond, W.J., 2011. Deciphering the distribution of the savanna biome. New Phytol. 191, 197–209.
Liu, Z., Ballantyne, A.P., Cooper, L.A., 2019. Biophysical feedback of global forest fires on surface temperature. Nat. Commun. 10, 214.
Lizundia-Loiola, J., Otón, G., Ramo, R., Chuvieco, E., 2020. A spatio-temporal active-fire clustering approach for global burned area mapping at 250 m from MODIS data. Remote Sens. Environ. 236, 111493.
Lundberg, S.M., Lee, S.-I., 2017. A unified approach to interpreting model predictions. In: Proceedings of the 31st International Conference on Neural Information Processing Systems. Curran Associates Inc., Long Beach, California, USA, pp. 4768–4777.
Malamud, B.D., Morein, G., Turcotte, D.L., 1998. Forest fires: an example of self-organized critical behavior. Science 281, 1840–1842.
Markham, C.G., 1970. Seasonality of precipitation in the United States. Ann. Assoc. Am. Geogr. 60, 593–597.
Mondal, N., Sukumar, R., 2016. Fires in seasonally dry tropical forest: testing the varying constraints hypothesis across a regional rainfall gradient. PloS One 11, e0159691.
Montfort, F., Nourtier, M., Grinand, C., Maneau, S., Mercier, C., Roelens, J.-B., et al., 2021. Regeneration capacities of woody species biodiversity and soil properties in Miombo woodland after slash-and-burn agriculture in Mozambique. For. Ecol. Manage. 488, 119039.
Nascimento, H.E.M., Laurance, W.F., 2002. Total aboveground biomass in central Amazonian rainforests: a landscape-scale study. For. Ecol. Manage. 168, 311–321.
Nikonovas, T., Spessa, A., Doerr, S.H., Clay, G.D., Mezbahuddin, S., 2020. Near-complete loss of fire-resistant primary tropical forest cover in Sumatra and Kalimantan. Commun. Earth Environ. 1.
Oom, D., Silva, P.C., Bistinas, I., Pereira, J.M.C., 2016. Highlighting biome-specific sensitivity of fire size distributions to time-gap parameter using a new algorithm for fire event individuation. Remote Sens. (Basel) 8.
Ordway, E.M., Asner, G.P., 2020. Carbon declines along tropical forest edges correspond to heterogeneous effects on canopy structure and function. Proc. Natl. Acad. Sci. 117, 7863–7870.
Padilla, M., Stehman, S.V., Chuvieco, E., 2014. Validation of the 2008 MODIS-MCD45 global burned area product using stratified random sampling. Remote Sens. Environ. 144, 187–196.
Pausas, J.G., 2019. Generalized fire response strategies in plants and animals. Oikos 128, 147–153.
Pausas, J.G., Bradstock, R.A., Keith, D.A., Keeley, J.E., 2004. Plant functional traits in relation to fire in crown-fire ecosystems. Ecology 85, 1085–1100.
Pellegrini, A.F.A., Ahlström, A., Hobbie, S.E., Reich, P.B., Nieradzik, L.P., Staver, A.C., et al., 2018. Fire frequency drives decadal changes in soil carbon and nitrogen and ecosystem productivity. Nature 553, 194–198.
Poorter, L., Mcneil, A., Hurtado, V.-H., Prins, H.H.T., Putz, F.E., 2014. Bark traits and life-history strategies of tropical dry- and moist forest trees. Funct. Ecol. 28, 232–242.
Potapov, P., Turubanova, S., Hansen, M.C., Tyukavina, A., Zalles, V., Khan, A., et al., 2022. Global maps of cropland extent and change show accelerated cropland expansion in the twenty-first century. Nat. Food 3, 19–28.
Ramo, R., Roteta, E., Bistinas, I., van Wees, D., Bastarrika, A., Chuvieco, E., et al., 2021. African burned area and fire carbon emissions are strongly impacted by small fires undetected by coarse resolution satellite data. Proc. Natl. Acad. Sci. 118, e2011160118.
Reiner, F., Brandt, M., Tong, X., Skole, D., Kariryaa, A., Ciais, P., et al., 2023. More than one quarter of Africa's tree cover is found outside areas previously classified as forest. Nat. Commun. 14.
Roteta, E., Bastarrika, A., Padilla, M., Storm, T., Chuvieco, E., 2019. Development of a Sentinel-2 burned area algorithm: generation of a small fire database for sub-Saharan Africa. Remote Sens. Environ. 222, 1–17.
Rudel, T.K., 2013. The national determinants of deforestation in sub-Saharan Africa. Philos. Trans. R. Soc., B 368, 20120405.
Rudel, T.K., Defries, R., Asner, G.P., Laurance, W.F., 2009. Changing drivers of deforestation and new opportunities for conservation. Conserv. Biol. 23, 1396–1405.
Santoro, M., Cartus, O., 2021. ESA Biomass Climate Change Initiative (Biomass_cci): Global Datasets of Forest Above-ground Biomass for the Years 2010, 2017 and 2018. NERC EDS Centre for Environmental Data Analysis.
Sayer, J.A., Harcourt, C.S., Collins, N.M., 1992. The Conservation Atlas of Tropical Forests Africa. Palgrave Macmillan UK, London.
Scheper, A.C., Verweij, P.A., van Kuijk, M., 2021. Post-fire forest restoration in the humid tropics: a synthesis of available strategies and knowledge gaps for effective restoration. Sci. Total Environ. 771, 144647.
Schroeder, W., Oliva, P., Giglio, L., Csiszar, I.A., 2014. The New VIIRS 375 m active fire detection data product: algorithm description and initial assessment. Remote Sens. Environ. 143, 85–96.
Shapley, L.S., Arrow, K.J., Barankin, E.W., Blackwell, D., Bott, R., Dalkey, N., et al., 1953. A value for N-person games. In: Kuhn, H.W., Tucker, A.W. (Eds.), Contributions to the Theory of Games (AM-28), Volume II. Princeton University Press, pp. 307–318.
Stroppiana, D., Sali, M., Busetto, L., Boschetti, M., Ranghetti, Luigi, Franquesa, M., et al., 2022. Sentinel-2 sampling design and reference fire perimeters to assess accuracy of Burned Area products over Sub-Saharan Africa for the year 2019. Int. J. Photogrammetry Remote Sensing 191, 223–234.
Styger, E., Rakotondramasy, H.M., Pfeffer, M.J., Fernandes, E.C.M., Bates, D.M., 2007. Influence of slash-and-burn farming practices on fallow succession and land degradation in the rainforest region of Madagascar. Agr Ecosyst Environ 119, 257–269.
Tatem, A.J., 2017. WorldPop, open data for spatial demography. Sci. Data 4, 170004.
Taubert, F., Fischer, R., Groeneveld, J., Lehmann, S., Müller, M.S., Rödig, E., et al., 2018. Global patterns of tropical forest fragmentation. Nature 554, 519–522.
Taylor, C.M., Klein, C., Parker, D.J., Gerard, F., Semeena, V.S., Barton, E.J., et al., 2022. "Late-stage" deforestation enhances storm trends in coastal West Africa. Proc. Natl. Acad. Sci. 119, e2109285119.
Tritsch, I., Le Tourneau, F.-M., 2016. Population densities and deforestation in the Brazilian Amazon: new insights on the current human settlement patterns. Appl. Geogr. 76, 163–172.
Tyukavina, A., Hansen, M.C., Potapov, P., Parker, D., Okpa, C., Stehman, S.V., et al., 2018. Congo Basin forest loss dominated by increasing smallholder clearing. Sci. Adv. 4.
Tyukavina, A., Potapov, P., Hansen, M.C., Pickens, A.H., Stehman, S.V., Turubanova, S., et al., 2022. Global Trends of Forest Loss Due to Fire From 2001 to 2019. Front. Remote Sensing 3.

van der Werf, G.R., Randerson, J.T., Giglio, L., van Leeuwen, T.T., Chen, Y., Rogers, B.M., et al., 2017. Global fire emissions estimates during 1997–2016. Earth Syst. Sci. Data 9, 697–720.
Van Langevelde, F., Van De Vijver, C.A.D.M., Kumar, L., Van De Koppel, J., De Ridder, N., Van Andel, J., et al., 2003. Effects of fire and herbivory on the stability of savanna ecosystems. Ecology 84, 337–350.
van Wees, D., van der Werf, G.R., Randerson, J.T., Andela, N., Chen, Y., Morton, D.C., 2021. The role of fire in global forest loss dynamics. Glob. Chang. Biol. 27, 2377–2391.
Wooster, M.J., Roberts, G., Perry, G.L.W., Kaufman, Y.J., 2005. Retrieval of biomass combustion rates and totals from fire radiative power observations: FRP derivation and calibration relationships between biomass consumption and fire radiative energy release. J. Geophys. Res. 110.
Zhou, X., Wen, H., Zhang, Y., Xu, J., Zhang, W., 2021. Landslide susceptibility mapping using hybrid random forest with GeoDetector and RFE for factor optimization. Geosci. Front. 12.